Temperature modelling of the Dutch subsurface at the depth of the Dinantian

Report by SCAN

April 2020

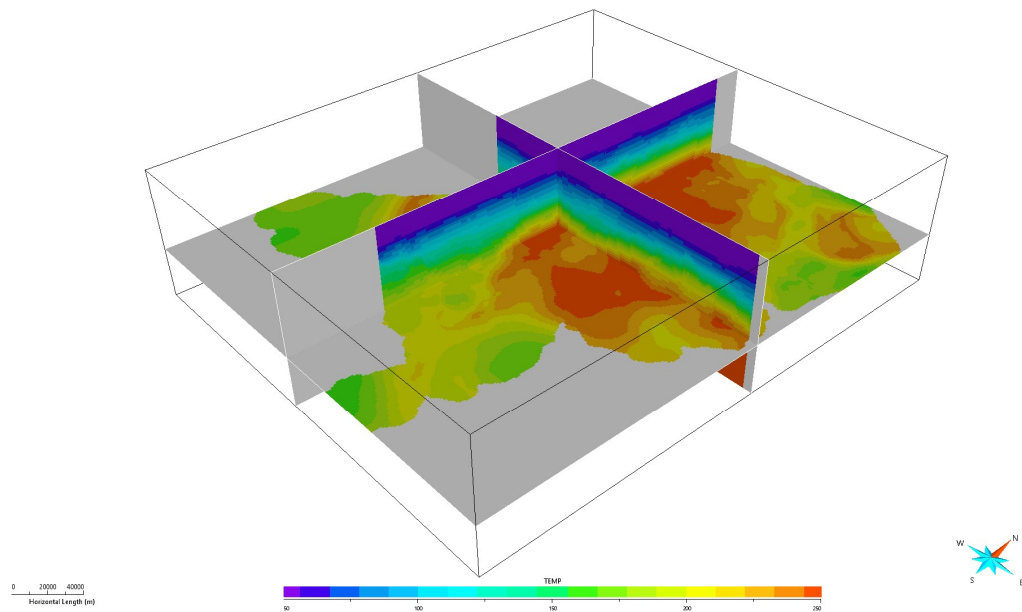# Temperature modelling of the Dutch subsurface at the depth of the Dinantian

Report written by

J.G. Veldkamp and D. Hegen

Applied Geoscience Group, Netherlands Organisation for Applied Scientific Research TNO, Princetonlaan 6, 3584 CB, Utrecht

April 2020

Dit rapport is een product van het SCAN-programma en wordt mogelijk gemaakt door het Ministerie van Economische Zaken en Klimaat

Table of Contents

List of figures and tables

Figures

Tables

Samenvatting en conclusies

In dit onderzoek is een bestaand temperatuurmodel van de Nederlandse ondergrond verder ontwikkeld met het oogmerk een betere schatting van de temperatuur van het Dinantien-gesteente te genereren. Een goed geschatte temperatuur op de diepte van het reservoir is een belangrijke parameter voor geothermische exploratie, aangezien het, onder andere, de business case bepaalt van de mogelijke geothermische toepassing. Temperatuur is daarnaast een belangrijke randvoorwaarde bij de keuze voor materialen en tools die gebruikt worden tijdens het boren en completeren van de put en tijdens de productiefase.

Het temperatuurmodel dat het onderwerp van deze studie is bestaat uit een driedimensionaal grid van de Nederlandse ondergrond. Relevante thermische eigenschappen (in waarde en onzekerheidsbandbreedte) worden aan alle onderscheiden lagen toegekend, inclusief aan de gesteenten van het Dinantien en het hierboven gelegen Namurien en Westfalien. De thermische eigenschappen omvatten de thermische conductiviteit en de radiogene warmteproductie. Een iteratieve rekenmethode wordt op het grid toegepast, waarbij de warmtevergelijking wordt opgelost, met conductie als dominant warmtetransportmechanisme. De berekende temperaturen worden hierna vergeleken met gemeten temperaturen. Vervolgens worden de vooraf gebruikte thermische eigenschappen en de warmtestroming iteratief bijgesteld om zo het verschil tussen de gemodelleerde en gemeten temperatuur te minimaliseren. Op deze wijze worden stapsgewijs temperatuurschattingen van de Nederlandse ondergrond gegenereerd die overeenkomen met de metingen, op basis van realistische schattingen van de thermische eigenschappen en de warmtestroming.

De workflow van de berekening wordt in dit rapport uitgelegd, evenals de relevante aspecten van de modellering uit vorige versies van het temperatuurmodel. Het gaat hierbij om de herkomst van het geologische lagenmodel, de temperatuurmetingen (type, toegepaste correctiemethoden, onzekerheden en bias), de achtergrond van de thermische eigenschappen van de lagen en de vraag of convectie als warmte-transportmechanisme voor het Dinantien in beschouwing moet worden genomen.

Om het verbeterde temperatuurmodel te maken zijn nieuwe gegevens gebruikt. De onderhavige studie maakt gebruik van verbeterde dieptekaarten van alle geologische eenheden, inclusief een geactualiseerde diepte van de top van het Namurien en van de top en dikte van het Dinantien. Nieuwe en soms betrouwbaardere temperatuurmetingen van het Dinantien en jongere lagen zijn gebruikt. In sommige boringen zijn in het Dinantien relatief hoge temperaturen gemeten. In de versie van het temperatuurmodel voorafgaand aan dit onderzoek werd convectie aangenomen als mogelijke verklaring van deze hoge temperaturen. In het temperatuurmodel dat in dit onderzoek is verder ontwikkeld worden deze temperaturen verklaard met behulp van betere inschattingen van de thermische conductiviteit van gesteenten van het Dinantien en de bovenliggende eenheden van Namurien- en Westphalien-ouderdom. Deze inschattingen zijn mede tot stand gekomen door gebruik te maken van een

nieuw faciesmodel van het Dinantien, waarmee ook de ruimtelijke verdeling van de thermische conductiviteit beter is bepaald. Op basis van nieuwe informatie over de reservoirkwaliteit van het Dinantien was het mogelijk te concluderen dat convectie geen rol speelt als warmtetransportmechanisme in het temperatuurmodel.

Het nieuwe temperatuurmodel voorspelt de temperaturen in het Dinantien beter dan het vorige temperatuurmodel. De verbeterde voorspellingen zijn onder meer mogelijk geworden doordat er meer temperatuurmetingen beschikbaar waren voor het Dinantien, en doordat gebruik is gemaakt van een nieuwe versie van het geologische lagenmodel. Ten opzichte van het vorige model voorspelt het nieuwe model hogere temperaturen in een groot deel van Nederland. Hiervoor zijn drie factoren aan te wijzen. Temperatuurmetingen uit het Dinantien die in het vorige model niet gebruikt werden tonen hogere temperaturen dan het vorige model voorspelde. Ten tweede is een nieuwe dieptekaart voor het Dinantien gebruikt, waarin het Dinantien in een groot deel van Nederland aanzienlijk dieper wordt geplaatst dan voorheen. Ten derde wordt de isolerende werking van de gesteenten die op het Dinantien liggen in het nieuwe model hoger ingeschat dan in het vorige temperatuurmodel, wat tot een hogere voorspelde temperatuur in het Dinantien leidt.

Aanbevelingen

Hoewel het huidige temperatuurmodel een grote verbetering is ten opzichte van het vorige model is er nog steeds ruimte voor verdere verbeteringen. Hiertoe kunnen verscheidene aanbevelingen voor toekomstig uit te voeren werk worden gedaan. Deze aanbevelingen, die in hoofdstuk 6 in detail uitgewerkt zijn, omvatten:

- Verwerken van de onzekerheid van de diepte van het Dinantien in het temperatuurmodel. Deze heeft een belangrijke invloed op de schatting van de temperatuur;
- Het verkrijgen van betere schattingen van de thermische eigenschappen van alle onderhavige gesteenten, door deze direct te meten aan gesteentekernen, deze indirect af te leiden uit geofysische logs, of door schattingen van de lithologie beter te gebruiken als proxy voor de eigenschappen;
- Het verzamelen en genereren van meer en betrouwbaardere temperatuurmetingen, de toepassing van een transparantere correctiemethode op de temperatuurmetingen, en beoordeling van een mogelijke bias en onzekerheid van de gebruikte correctiemethodes. De relevantie van de toepassing van glasvezelkabel voor temperatuurmetingen (DTS) wordt benadrukt. Bestaande putten die in de nabije toekomst opgeruimd zullen worden kunnen mogelijk gebruikt worden om dergelijke metingen uit te voeren tegen geringe meerkosten. Het wordt aanbevolen de technische en praktische haalbaarheid hiervan verder te evalueren. Ook zou de beschikbaarheid van evenwichts-temperatuurmetingen bij de Nederlandse geothermie-, olie- en gasoperators kunnen worden nagegaan.

Sommige aanbevelingen zijn generiek van aard, en niet specifiek van toepassing op het Dinantien.

Executive summary and conclusions

In this study an existing temperature model of the Dutch subsurface has been further developed to predict the temperature of the Dinantian. A well estimated temperature at the depth of the reservoir is an important parameter for geothermal exploration as it determines, among other things, the business case of the possible geothermal application. It also serves as an important boundary condition for materials and tools to be used during drilling, completion and production.

The temperature model that is the subject of this study consists of a three-dimensional grid representing the Dutch subsurface. Relevant thermal properties (values and uncertainty range) are assigned to all layers, including the Dinantian and the overlying Westphalian and Namurian rocks. These thermal properties mainly concern thermal conductivity and radiogenic heat production. An iterative calculation procedure is performed on the grid, solving the heat equation with conduction as dominant heat exchange mechanism. Following each iteration temperature results are compared to measured subsurface temperatures. The thermal properties and heat flow are then adjusted iteratively in order to minimize the difference between the temperature observations and the modelled temperature. Thus, the stepwise calculation procedure arrives at resulting temperature estimates for the Dutch subsurface which fit the temperature measurements, based on realistic values for the thermal properties and heat flow.

In this report the workflow for this iterative procedure is explained first, discussing the modelling aspects that were covered in the prior version of the temperature model. These concern the representation of geology, the temperature measurement data (specific type, correction methods applied, uncertainties and bias involved), background on the thermal properties and whether or not to include convection as a heat transport mechanism for the Dinantian.

New data was used to generate the enhanced temperature model in this study. The current study relied on improved maps of all geological units, including an updated depth of the top of the Namurian, and on updated maps of the top and bottom depth of the Dinantian reservoir. Furthermore, reliable (and new) subsurface temperature measurement data (relevant for and partly covering the Dinantian and Namurian layers) was used. Relatively high temperatures were measured in rocks of Dinantian age in some wells. In the prior version of the temperature model the occurrence of convection was assumed as explanation high temperatures in the Dinantian. In the new temperature model these are explained by assuming a higher thermal conductivity of the rocks of the Dinantian, and a lower thermal conducty for the overlying units of Namurian and Westphalian age. These assumptions are supported by using a new facies model of the Dinantian, which also allowed to better determine the spatial distribution of thermal conductivities. Using new information about the reservoir quality of rocks of the Dinantian it was concluded that heat transport through convection does not play a role as dominant mechanism for heat transport in this unit.

The new temperature model is considered a major improvement at the depth of the Dinantian in comparison to the prior version of this model. This is mainly because of all the specific modelling for the Dinantian and additional relevant measurement data is accounted for. The temperatures obtained for the depth of the Dinantian are higher in the largest part of the Netherlands than the ones obtained with the prior model. The main reason for this being that the depth of the Dinantian reservoir is deeper than before. A further reason for these high temperatures may lie in the insulating nature of the layers overlying the Dinantian rocks.

Recommendations

Although a major improvement was achieved in the temperature modelling for the Dinantian rocks in the Dutch subsurface there is still considerable room for improvement. Recommendations are therefore made for further work. These recommendations are described in technical detail in Chapter 6. In summary these concern:

- Accounting for the uncertainty of the depth of the Dinantian reservoir in the temperature model, which may have a significant impact on the temperature estimate;
- Obtaining better estimates of the thermal properties of all rocks involved via direct measurement of these properties on core material, estimation from well logs, and use of lithology as proxy estimator;
- Collection and generation of more reliable temperature measurements, application of more transparent correction methods to such data and assessment of the potential bias of such methods. The relevance of application of fibre optic technology for temperature measurement (DTS) is emphasized. Many existing wells that will be abandoned in the near future could be used to obtain such measurements at limited additional cost. Furthermore, the availability of temperature data among Dutch operators (in the geothermal and hydrocarbons production sectors) could be checked.

Some of these recommendations are generic in nature and do not apply to the Dinantian only.

1 Introduction

Geothermal energy systems may contribute significantly to the transition to a sustainable energy system in The Netherlands. More than 20 geothermal systems are currently in operation in the Netherlands, which are mainly used for the heating of greenhouses. These systems produce from intermediate (2 to 3 km) depth, at temperatures up to about 100 ºC. For some types of heat demand, for instance in the process industry, higher temperatures are required. These temperatures are found in the subsurface at depths exceeding four kilometres. When heat is produced from these depths this is referred to as Ultra Deep Geothermal (UDG). The Dutch subsurface has not been explored extensively at these depths until now and is therefore relatively unknown. Based on limited subsurface data, the Lower Carboniferous Dinantian Carbonates were identified by [Boxem et al. (2016)] as the most promising target matching the requirements for UDG.

The reservoir temperature is a crucial parameter for geothermal installations, as it determines the potential application (e.g. direct use vs. steam generation), and the business case (more heat likely generates more revenue). This temperature also dictates what materials and tools can or should be used during drilling, completion and production. Furthermore, the reservoir temperature also plays a role in assessing the seismic risk.

As the reservoir temperature is a key parameter for geothermal exploration and production, it is important to estimate the temperature at all relevant depths in the subsurface by means of a so-called temperature model. Such a temperature model is defined here as a three-dimensional grid representing the Dutch subsurface and for which via a calculation procedure a temperature estimate is obtained for each grid cell. Three models for the Dutch subsurface were made previously. They are described in [Bonté et al. (2012); Struijk (2016); Békési et al. (in prep.)].

This report documents a study with the objective to improve the estimation of temperatures in the Dinantian carbonates of the Dutch subsurface. Until recently, relatively little attention was paid to the temperature modelling of the Dinantian because of the scarcity of available data for the depths of interest. The study is part of SCAN, a government funded program to scope out the potential of geothermal energy, including the Dinantian Carbonates, which consists of, amongst others, a range of subsurface studies of the Dinantian Carbonates. Results of the SCAN studies are and will further become available via www.nlog.nl/scan.

For the study the temperature model for The Netherlands has been enhanced using new and updated versions of relevant input data as generated in the SCAN program. Those data include:
- Temperature measurements
- Structural model and reservoir properties for the Dinantian Carbonates

The enhancements to the temperature model and the results obtained for the Dinantian are the subject of this report, which has the following set-up. Chapter 2 describes the generic set-up of the temperature model. The data and modelling assumptions on which the temperature model is based, prior to the current study, are discussed in chapter 3. The enhanced temperature model is subject of chapter 4. This chapter focuses amongst others on the new data that has become available in several SCAN studies, and which is used in this study. Chapter 5 discusses the results obtained for the Dinantian with the enhanced temperature model. The last chapter presents the conclusions of the study and provides suggestions for future work. The report is complemented with references and three appendices serving the reader with several displays in a larger format.

2 Set-up of the prior temperature model for the Dutch subsurface

A first version of 3D temperature model for the Dutch subsurface was accomplished in 2012 and published by Bonté et al. (2012). It has been updated in several steps since then to establish the last version from 2018 as described by Békési et al. (in prep.). The set-up of such a 3D high resolution temperature model is not trivial. The associated workflow calculations, computer coded in JAVA, require significant calculation time and are computer memory intensive. The temperature model workflow, therefore, consists of several steps where each relies on the previous one. The steps are:

1. Coarse scale 3D grid model with multi-1D thermal calculations
2. Coarse scale 3D grid model with 3D thermal calculations
3. Estimation of radiogenic heat production
4. Estimation of vertical thermal conductivity
5. High-resolution 3D model with multi-1D thermal calculations
6. High-resolution 3D model with 3D thermal calculations
7. Reflection of cooling effect of glaciations
8. Estimation of vertical thermal conductivity and resulting temperature distribution estimate

These eight steps are further described in the next two sections. This chapter concludes with a section on the inversion procedure applied in several of the workflow steps.

2.1 Coarse scale 3D grid model

2.1.1 Step 1. Coarse scale grid and multi-1D thermal calculations

A coarse scale 3D grid model is built which has a spatial resolution of 3000 by 3000 metre in the horizontal plane. The vertical spatial resolution is 200 metre down to a depth of 10 kilometre, and 3000 metres further down to a depth of 100 kilometre. The resulting multi-layer model for the Dutch subsurface includes the lithospheric mantle, the lower crust and the upper crust. The latter is split into 14 sedimentary layers of Palaeozoic through Quaternary age. It is built using the DGM-Deep geological model of the Netherlands. More background on this model, which is available at www.nlog.nl, will be given at the beginning of the next chapter.

A 3D temperature model describes, at each areal location, the vertical temperature profile. The temperature gradient (°C/m or similarly °K/m) defining this profile is defined as the heat flow (W/m^2) divided by the vertical thermal conductivity (W/mK). Therefore, a correct estimation of the latter two properties is key for obtaining a proper temperature model. Initial thermal conductivity and authigenic heat production are assigned as main thermal rock properties to all layers using textbook estimates derived from [Hantschel & Kauerauf (2009)]. The bulk thermal

conductivity of a heterogenous volume of rock is a function of the contributing rock types, and pore water, at given temperature and pressure. Clastic rock thermal conductivities typically lie within a range from ~0.8 W/mK to ~6.5 W/mK (Figure 2.1). The thermal conductivity depends on temperature and pressure (e.g. explained in [Kukkonen et al. (1999)]). An increase in temperature reduces the thermal conductivity. Increasing pressure, due to burial, reduces the porosity (compaction) which replaces water by rock in the bulk rock volume, thereby increasing the bulk thermal conductivity[1]. Hence, the initially assigned thermal conductivities are corrected for burial using porosity-depth relationships.

After having assigned the main thermal rock properties the heat equation is solved for each vertical stack of grid cells for each horizontal grid location in this layer model. This solution is referred to as multi-1D thermal calculations. The boundary conditions for all these 1D calculations concern a temperature of 8 °C, at surface level[2] and one of 1200 °C at 100 kilometres depth ([Limberger & Van Wees (2014)], [Tesauro et al. (2009)]). This yields initial values for temperature, thermal conductivity and the authigenic heat production at each grid cell in the 3D model, which agree with first order estimates.

2.1.2   Step 2. Coarse scale grid and 3D thermal calculations

Based on the default properties obtained in the previous step a starting 3D temperature distribution for the grid is determined based on solving the heat equation in 3D, i.e. in one solution procedure for the entire 3D grid. This solution procedure differs from the multi-1D approach of the previous step. In this current step, the model is not yet fitted to any temperature measurements. Therefore, there are misfits between measured and calculated temperatures.

---

[1] The effect of pressure alone on thermal conductivity is very limited

[2] In [Bonté et al. (2012)] a surface temperature of 10 °C is proposed, which is in agreement with the current average surface temperature of the Netherlands. Because the subsurface temperature is currently not in equilibrium with the surface temperature as a result of the various age ages in the last ~150,000 years and the Holocene warm period since ~10,000 years, a better fit with measured temperatures in the shallow subsurface up to ~2 kilometre is obtained using a surface temperature of 8 °C.
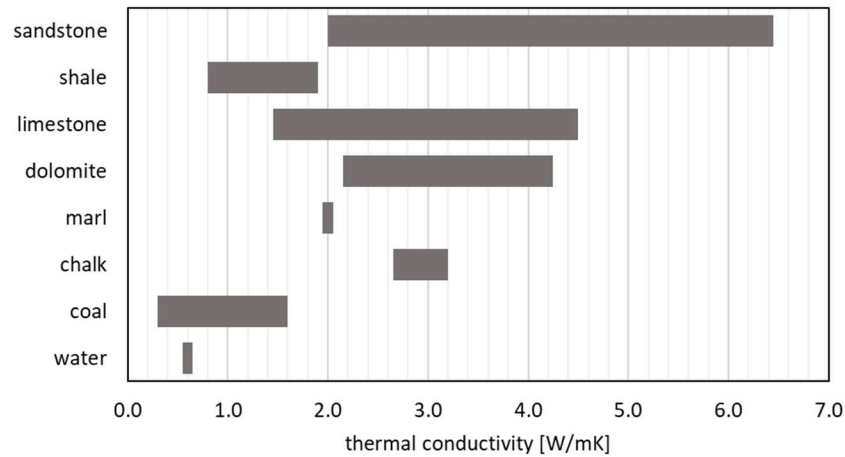
Figure 2.1   Typical rock thermal conductivity ranges from [Hantschel & Kauerauf (2009)] and water, at ambient conditions. See Table 3.2 and Table 3.3 for more detailed information on rock thermal conductivities.

This coarse scale gridded model is fitted to temperature measurements in the next two steps.

2.1.3   Step 3. Estimation of radiogenic heat production

As a next step the prior estimate of radiogenic heat production (A) in the upper crust, obtained in step 1, is updated via an inversion procedure known as Ensemble Smoother with Multiple Data Assimilation (ES-MDA). This technique is described in more detail in [Emerick & Reynolds, (2013)].

In this procedure the main results of several representations of the coarse 3D model (each representing uncertainty in the model property A), being the temperature distribution, are compared with observed (i.e. measured) subsurface temperatures and which the observations also have a certain uncertainty. The estimates for the radiogenic heat production are adjusted repeatedly on basis of the comparisons between calculated and measured temperatures on different locations in the 3D layered model, and the uncertainties involved. The is fixed at the top and the bottom of the model, the heat flow is allowed to vary. This procedure is continued until no further improvements is obtained between the modelled and measured temperatures.

2.1.4   Step 4. Estimation of vertical thermal conductivity

The results of step 3 are subject of a next ES-MDA inversion procedure aiming to update the prior estimate (as obtained in step 1) of the vertical thermal conductivity (KV) in the sedimentary layers. In the inversion procedure the temperature distributions as calculated for the coarse 3D model are compared to measured temperatures in the subsurface, in a similar fashion as was explained for step 2.

These measured temperatures are obtained from measurements taken in boreholes during or after drilling. Section 3.2 provides further background on those measurements.

16

2.2 High-resolution 3D grid model

The coarse 3D grid and the results obtained in four workflow steps discussed in section 2.1 are used in subsequent workflow steps. In these steps, calculations are performed on a high-resolution 3D grid representation of the Dutch subsurface.

2.2.1 Step 5. High-resolution 3D grid and multi-1D thermal calculation

The coarse 3D grid is further refined to a high-resolution grid representation with a resolution of 1000 metre by 1000 metre in the horizontal plane and a vertical resolution of 200 metre down to a depth of 10 kilometres. A heat flow (lower) boundary condition is now applied at 10 kilometres depth, which is derived from step 4 of the workflow. Furthermore, again a constant surface temperature of 8 °C is applied. This grid representation is used to perform multi-1D model thermal calculations, similar to step 1. The updated thermal properties authigenic heat production (A) and vertical thermal conductivity (KV) as obtained from the steps 3 and 4 are used.

2.2.2 Step 6. High-resolution 3D grid and 3D thermal calculation

Similar to step 2 of the workflow, the results obtained for the high-resolution 3D model in step 5 are used to further determine a temperature distribution for the grid based on solving the heat equation in 3D.

2.2.3 Step 7. Reflection of cooling effect of the glaciations

The results obtained in step 6 are used in a subsequent step to account for (and reflect in the temperature model) the cooling effect of the glaciations that occurred between 150,000 years ago and present day [Gies (2019)]. This violates the assumption that the current temperature distribution in the subsurface is in steady state as the shallow subsurface is still slowly reheating. This effect is introduced by using estimates of the paleo-surface temperature in order to mimic the cooling by lowering the authigenic heat production.

2.2.4 Estimation of vertical thermal conductivity and resulting temperature distribution

The final work flow step for the temperature model updates the vertical thermal conductivity (KV) of the sediments as represented in the high-resolution 3D grid, again via an inversion procedure applying ES-MDA and using measured temperatures.

A final temperature distribution has been obtained for the 3D grid representing the Dutch subsurface after completion of this calculation procedure.

2.3 Setting rock properties for the inversion procedure

Several of the workflow steps of the temperature model involve application of ES-MDA for inversion of the key rock properties thermal conductivity and authigenic heat production, and of the heat flow. In such a procedure these properties are modified in order to obtain a better match between the modelled and the measured (observed) temperatures. The rock properties are allowed to change within user specified limits, using a uniform or triangular distribution, or a shift. It is important for the temperature model to allow for a variation of the rock properties in a sufficiently wide range. A good fit between observed and modelled temperatures cannot be obtained when the specified range is too small. If the range is set too wide on the other hand, unrealistic rock property values may result. The changed property can be applied on spatial scale of the entire grid of the temperature model (bulk shift, specified per layer), or locally, via a user specified spatial range of influence.

3 Main modelling aspects for the Dinantian in the prior temperature model

The construction of a proper temperature model for the Dutch subsurface which sufficiently accurately accounts for the Dinantian has been challenging until now because of the following aspects:

- Both the depth and thickness of the Dinantian reservoir are poorly constrained in a large part of the Dutch subsurface;
- Only a few reliable temperature measurements exist for the Dinantian. Furthermore, some of the available temperature measurements suggest temperatures in the Dinantian that are higher than would be expected from the average gradient published by [Bonté et al. (2012)], but the underlying mechanism is not fully understood;
- The facies of the Dinantian, and therefore the rock type and the relevant rock thermal properties, are not well known;
- The permeability is not well known. This property is important because it determines, among other factors, whether conduction or convection is the dominant heat transport mechanism is.

As a result, the modelling of the temperature of the Dinantian rocks has a certain degree of uncertainty. More accurate knowledge of the above-mentioned aspects is key for improved and accurate modelling, and better understanding of the temperature distribution in the Dinantian. This chapter describes how the challenges related to the aspects described above have been addressed for the prior (2018) version of the temperature model (as described by [Békési et al. (in prep.)]). Each of the above aspects is the subject of a separate section.

3.1 Geological modelling

The uppermost part in the 3D grid representation of the prior temperature model has been constructed from the DGM-Deep v4 geological model (www.nlog.nl/en/geological-maps).

> DGM-Deep (Digital Geological Model) is a 2.5D stacked layer geological model of the Dutch subsurface. It is based on a combination of interpreted 3D and 2D seismic data and wells. The VelMod 3.1 model was used for converting the interpreted horizons from time to depth. It is regularly updated. DGM-Deep v4 (2014) was used for the prior version of the temperature model. DGM-Deep v5 became available late 2019 and was used for the enhanced temperature model (see section 4.3).

DGM-Deep v4 contains layers down to the base of the Carboniferous Limburg Group (DC). A very rough estimate of 700 metre has been used as thickness for the entire Dinantian succession in the 3D grid representation. A separate layer has been added representing the base of the Paleozoic (Silurian) which overlies the London

Brabant Massive in the southern part of the country. The 3D grid contains 14 sedimentary layers listed in Table 3.1. Figure 3.1 shows a generalized cross section through the Netherlands on geological Group level showing the layers present in DGM-Deep v4.

The deepest layer of the DGM-Deep v4 model is the base of the Limburg Group, which is represented by the layers 10 and 11 of Table 3.1. Figure 3.1 shows the Limburg Group as the deepest interpreted layers. The depth of this layer exceeds 8000 metres in Noord-Brabant (Roer Valley Graben area), Eastern Drenthe and in North-Eastern Friesland (Lauwerszee Trough). At these locations the interpreted depth is speculative because reflectors representing the base of the Limburg Group are difficult or impossible to identify, or because seismic data are unavailable. The base of the Limburg Group, which corresponds to the top of the Dinantian, is found at very shallow depth in Zeeland and Southern and Northern Limburg, where the depth is less than several hundreds of metres. As can be observed from Figure 3.1, the maximum depth at which the DGM Deep v4 model provides information varies considerably throughout the Netherlands. Especially in the Southern part of the country, the deepest interpreted horizons are found at shallow depth.

Table 3.1   Layers in the geological model, based on DGM-Deep v4 model. Colours correspond to the layers in Figure 3.1.

model layer number	unit	DGM-Deep code
1	Upper North Sea Group	NU
2	Lower and Middle North Sea Group	NLNM
3	Chalk Group	CK
4	Vlieland Group	KN
5	Schieland Group	S
6	Altena Group	AT
7	Triassic Group	RBRN
8	Zechstein Group	ZE
9	Rotliegend Group	RO
10	Caumer/Dinkel/Hunze Subgroups (Westphalian)	DCC/DCD/DCH
11	Geul Subgroup (Namurian)	DCG
12	Carboniferous Limestone (platform)	CL
13	Carboniferous Limestone (non-platform)	CL
14	Base Paleozoic (Zeeland area)	
-1	Upper Crust	
-2	Lower Crust	
-3	mantle	-
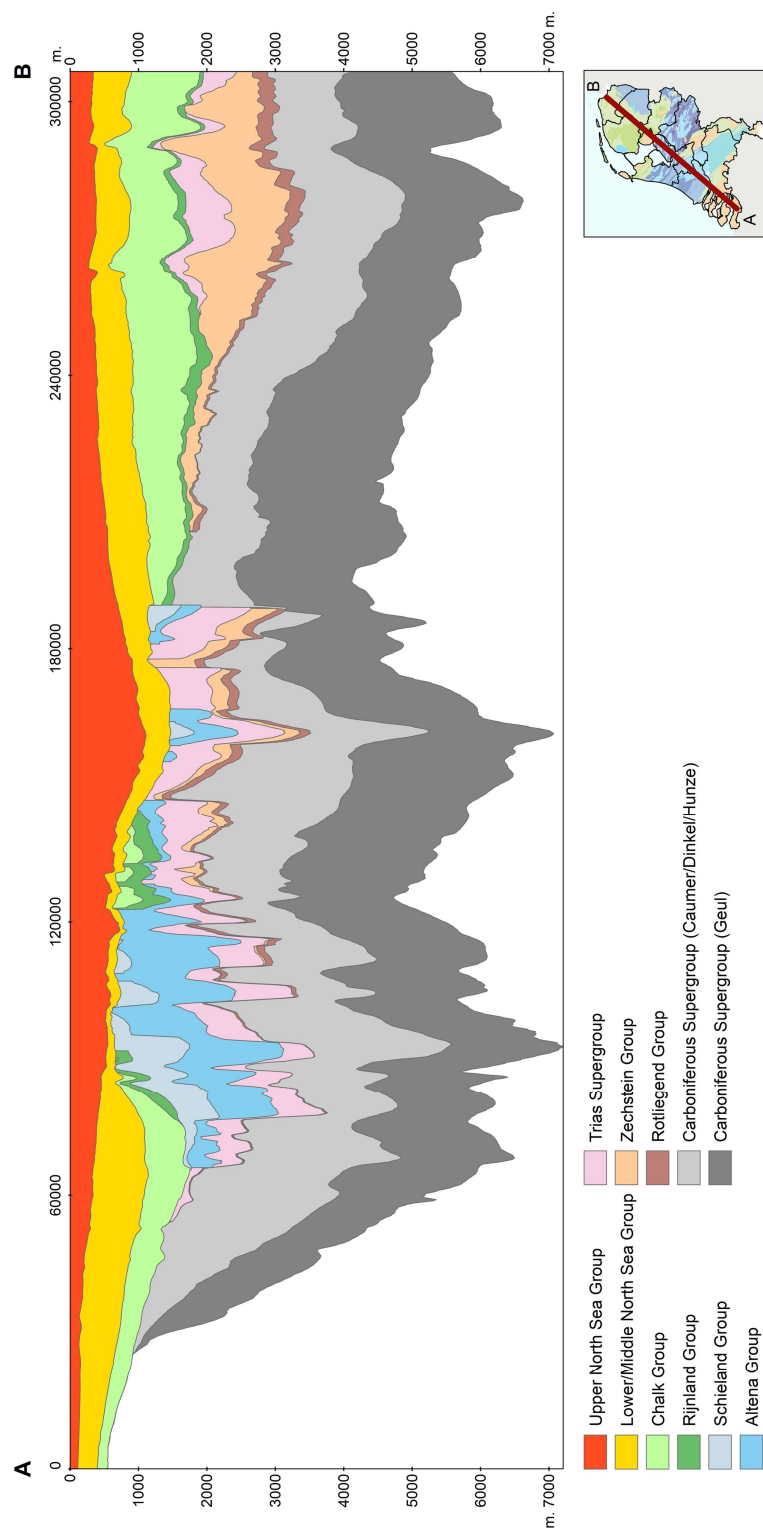
Figure 3.1   Generalized cross section through the Netherlands based on DGM-Deep
v4 model.

3.2 Temperature measurement data[3]

Temperature measurement data is a very important input of the temperature model, as became clear from the workflow description in the previous chapter. Therefore, a database of ~1500 subsurface temperature measurements is used for the model. This database is available www.nlog.nl/en/temperature-data. Most measurements in this dataset have been extracted from scanned well logs and well and logging reports. This measurement data is spread heterogeneously over the country, with an emphasis on the Western and Northern parts, as is shown inFigure 3.2. Figure 3.3 shows the distribution of the measurements over the depth in the subsurface. From this distribution it can be seen that only 44 measurements are from a depth below four kilometres, and only three measurements from below a depth of five kilometres.

Temperatures are often measured routinely during drilling operations. The temperature is however seldomly recorded as main operation, but many logging tools are equipped with temperature sensors. Usually the recorded temperature is the maximum temperature that was reached during the logging. This type of temperature measurement is referred to as bottom hole temperature (BHT). Temperatures measured in this way are usually not the in situ subsurface temperatures. This is because in the deeper subsurface the near wellbore is being cooled by the drilling mud, and at shallow depths the drilling mud, which was heated in the deeper section of the well, heats the subsurface as illustrated in Figure 3.4 for the well DEW-05. A similar observation was made by NAM for the Zeerijp-3 well, where the shallow subsurface down to ~1500 metres was cooling and the deep subsurface down from ~2000 metres reheating during the first three months of temperature monitoring (figure 4.1 in [Cannon & Kole (2018)]).

Before an accurate temperature measurement can be done, the reservoir temperature needs to return to equilibrium after the drilling operations and mud circulation have ceased. This may take a considerable amount of time. Equilibrium is rarely reached because the operations usually resume long before such equilibrium is established. Relevant operational data that are sometimes displayed on the logs are the maximum recorded temperature, the drill bit diameter, the depth of the logged interval, and, sometimes, the time since circulation of drilling fluids stopped. Figure 3.5 shows an example.

The database with temperature measurements as used in the temperature model consists of various types of measurements. All have different accuracies and biases and should therefore be treated differently. These various types of measurement are described in the remainder of this section.

---

[3] This section was co-authored by Marten ter Borgh
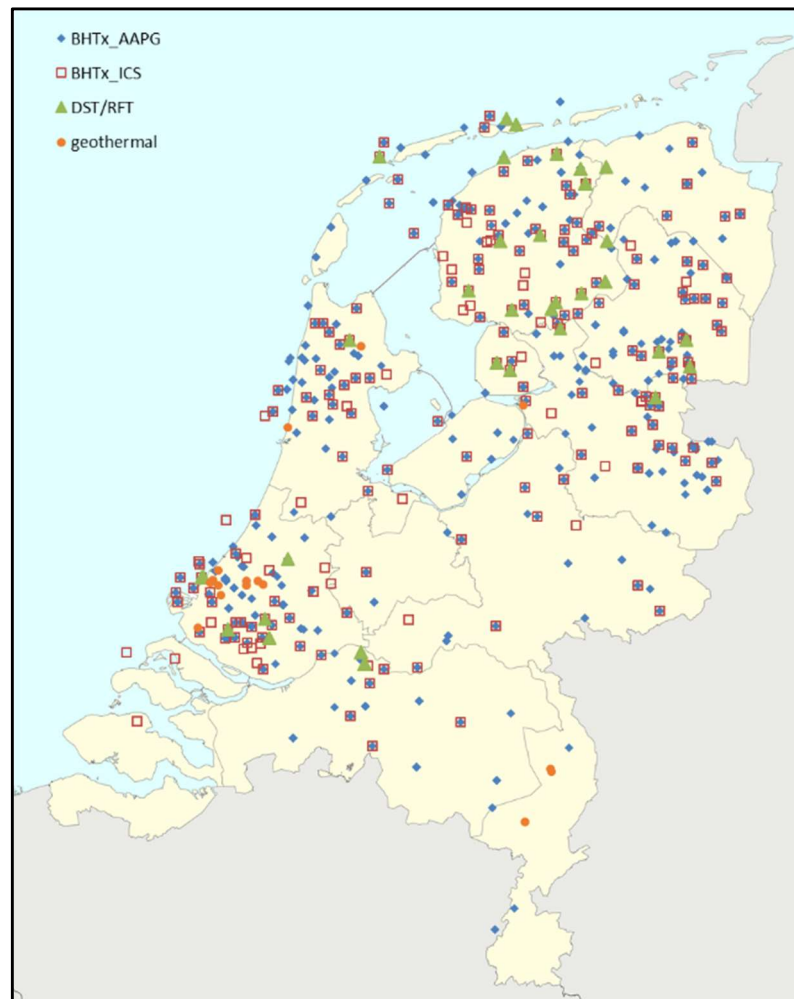
Figure 3.2   Distribution of temperature measurements.
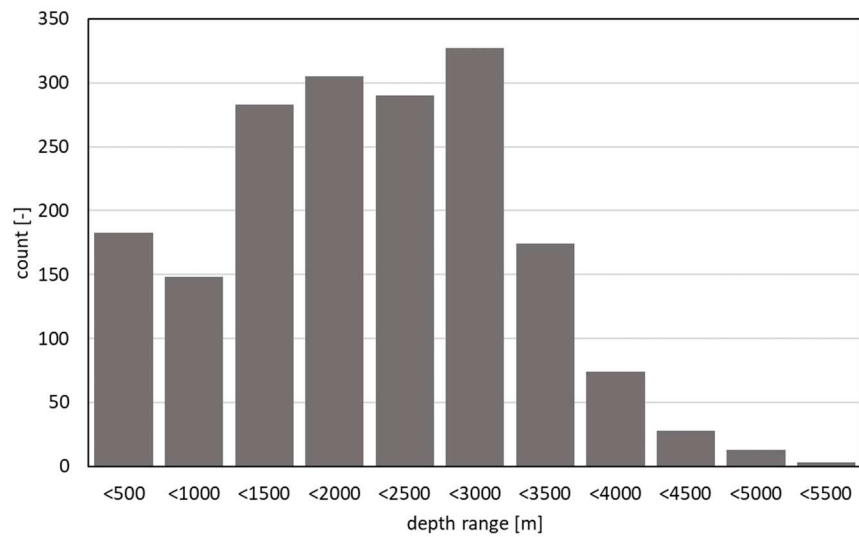
Figure 3.3   Depth distribution of the temperature measurements.
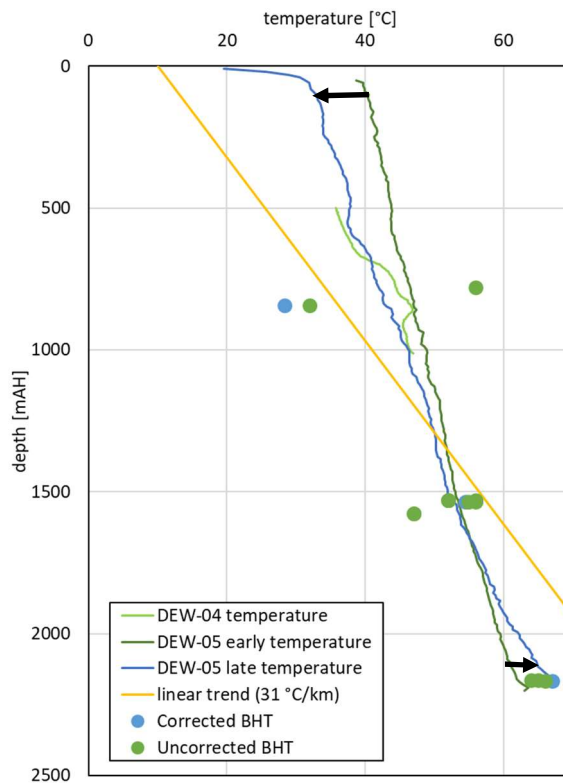
Figure 3.4   Early (dark green) and late (blue) temperature logs of the Deurninge-Weerselo 5 well show the effect of shallow heating and deep cooling. Arrows indicate change direction of temperature development towards equilibrium.

Figure 3.5   Example of bottom hole temperature data in the well ZRP-01.

3.2.1 Geothermal doublet temperatures

For geothermal operations, temperature is one of the most important variables, and is therefore measured accurately and over longer periods. In the database temperature data is available for 16 doublets. These temperatures are considered to represent the true reservoir temperature. It should be noted, however, that publishing temperature data is not a legal requirement for operators, and that measuring and reporting protocols have not been standardized. Inaccuracies may therefore be a result.

3.2.2 Drill stem and repeat formation tests

Temperatures can be derived accurately from Drill Stem Tests (DST) and Repeat Formation Tests (RFT) data. Most DST available in the database were copied from the Integrated Pressure Information System of the Netherlands (Pressure SNS, [Verweij & Hegen (2015)]). Most of the data, including DST and RFT data, in Pressure SNS has been given a coding for quality/reliability classification. The standard deviation can be about 1.5 °C if the results from different DST on the same structure are compared. [Hermanrud et al. (1991)] argue that deriving a good quality temperature estimate from DSTs is not trivial. Various factors are known to affect the temperature, such as:

a) cooling or heating during testing due to mud circulation;
b) duration of the flow period; the temperature rises rapidly at the start of a flow period and then levels out toward equilibrium;
c) secondary thermal effects such as distance between sensor and perforated interval, lag time of recorded temperature, fluid compression after shut-in;
d) vertical heat conduction in casing and test string;
e) frictional heating from moving fluids.

Any inaccuracies caused by the above-mentioned factors usually lead to an underestimation bias of the virgin reservoir temperature. Because not all of the above-mentioned factors are always well known, we assigned a maximum error of ±8 °C to this type of measurements instead of the 1.5 °C that can in principle be achieved. It should be noted that this permits the model more flexibility in estimating local temperatures, but this may not compensate for the possible underestimation bias. 65 measurements of this type are currently available in the temperature measurements database.

3.2.3 Bottom hole temperatures

It is possible to correct measured non-equilibrium bottom hole temperatures (BHT) when these are measured multiple times at the same depth and at different moments after the mud circulation has stopped. In [Goutorbe et al. (2007)] various correction techniques are applied on a large Australian data set consisting of over 650 groups of BHT measurements. In this publication it is concluded that extrapolated undisturbed temperatures as obtained for all the methods are qualitatively in agreement (i.e. within 5–10 °C) with measurements from drillstem tests for most of the wells. However, a graphical plot of the data of this publication as found in Figure 3.6 shows

that there is a tendency for temperatures corrected using relatively simple methods (such as the ICS and AAPG method used in this study) to be biased towards lower temperatures, especially when the time after the stop of mud circulation is relative small. Based on a limited series of measurements, in [Hermanrud et al. (1990)] it is stated that more advanced correction methods produce results that are close to DST measurements and which are unbiased, but with errors up to ±9 °C. These advanced correction methods require input data that is generally not available. These methods have therefore not been used so far for the Dutch temperature model. [Hermanrud et al. (1990)] also conclude that even simpler methods such as the ones used here produce temperatures that are too low.

The Horner correction method requires the least amount of data, specifically only the mud circulation time t. The method uses a regression of temperature against a derivative of time, i.e. log10(t+dt)/dt where dt is the time after stop of circulation. For accurate estimations, according to [Peters & Nelson, (2009)] application of the Horner method also requires:

- availability of a minimum of 3 logging runs that record both time and temperature;
- an extrapolation of temperature less than the range of temperature data;
- the deviation from the least squares regression line to be less than the measurement uncertainty (1-3 °C).

[Goutorbe et al. (2007)] conclude that Horner temperature predictions are systematically lower when the underlying approximations do not hold anymore, which they state, is when

$$a^2/4\kappa_r t_e \geq 1 \qquad\qquad (3.1)$$

With:

      a = borehole radius
      κ_r = rock thermal diffusivity (thermal conductivity divided by density and specific heat capacity)
      t_e = elapsed time after heat release (i.e. after circulation stopped)

The result of equation (3.1) may exceed a (dimensionless) value of 1 when the borehole radius is too large or the elapsed time too small. Additionally, [Shen & Beck, (1986)] point out that a Horner plot may yield unreasonable predictions of the equilibrium formation temperature when BHTs are measured at small shut-in times.

For the Horner correction it can be concluded that the resulting accuracy is ±8°C, where the method is considered in [Hermanrud et al. (1990)] to be less advanced and biased towards lower temperatures. This is confirmed in [Waples & Pedersen, (2004)] where a set of data in the Danish Central Graben was evaluated and where it was found that the Horner corrected temperatures were consistently lower than the true temperature.
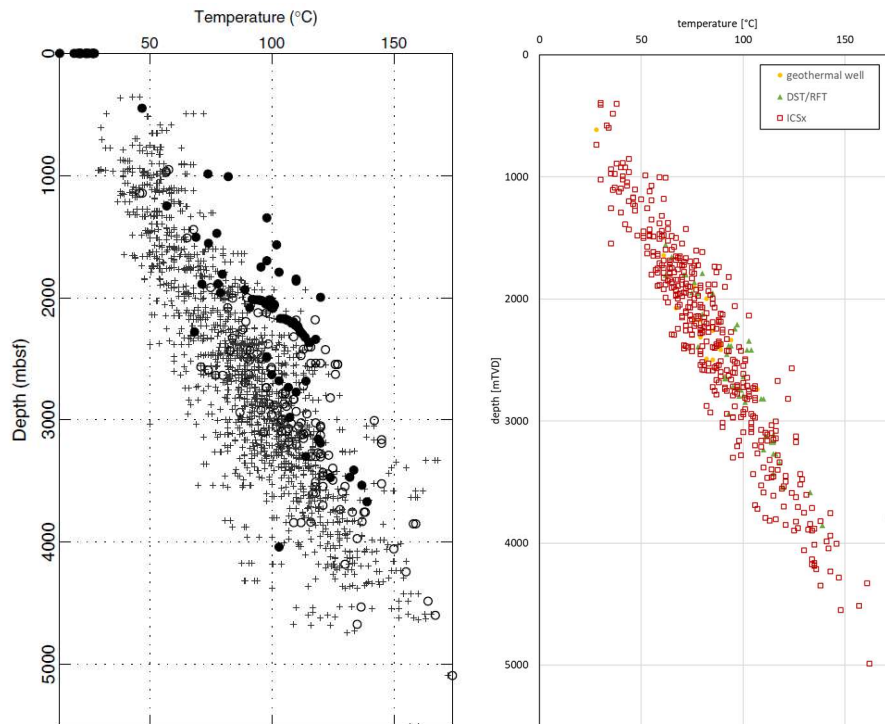
Figure 3.6   Left: temperate dataset used in [Goutorbe et al. (2007)] showing that BHT with relative small time since stop of mud circulation (crosses) underestimate the DST temperatures (black dots) more than BHT with longer time since circulation (open circles). Right: for the Netherlands dataset the BHT (ICS corrected) also appear to underestimate the DST temperatures.

The Instantaneous Cylindrical Source (ICS) correction was used to correct the BHT in the database with temperature measurements. The method relies on a single parameter depending on thermal diffusivity (uncertain) and borehole radius (which is often known). The database contains 439 measurements of this type. Following [Goutorbe et al. (2007)] it is assumed that the maximum error after proper correction is about ±10°C, and that a bias towards lower temperatures may exist. The uncertainty is incorporated in the model, but as described previously for the DST this may not address the underestimation bias.

A correction based on operations and well data (like time since stop of circulation and hole diameter) is not possible when only a single non-equilibrium BHT measurement is available. Such measurement data is therefore only corrected statistically for the database in order to be in line with the more accurate BHT measurements using a technique proposed in [Blackwell & Richards (2004)]. This correction is referred to as the AAPG correction. Similar to [Bonté et al. (2012)], a second correction was then applied to remove the difference in trend between ICS and AAPG corrected data. The latter data type is the most abundant in the database and consists of 983 measurements. The error after correction is about ±15°C. As the ICS data is probably biased, and this bias has not been removed, a bias should also be expected in the data corrected using the AAPG method.

Non-equilibrium temperature logs are sometimes recorded over substantial intervals of the borehole trajectory. Several are available in the NLOG wells database. Their correction is challenging because of the lack of sufficient data like circulation time and time since circulation, hence they have not been unlocked yet.

3.2.4 Temperature data in deep Dinantian rocks

The most extensive set of deep BHT data in (and close to) Dinantian rocks was measured in the LTG-01 well, where two measurements were done in the Namurian and three in the Dinantian. These measurements reveal that the temperature gradient is high in the Namurian and low in the Dinantian. Therefore, the temperature at the top of the Dinantian is higher than expected from the point of view of an average geothermal gradient, which is often assumed from [Bonté et al. (2012)] to be ~0.031 °C/m in the Dutch subsurface. It also means that the temperature increase within the Dinantian is low. For the Luttelgeest location, the temperature at 4200 metres depth using an average gradient would have been about 140 °C, but the measured temperature is 187 °C. As anomalously high temperatures are advantageous for geothermal operations, it is important to understand the mechanism responsible for the anomalous gradient in Luttelgeest, and to know whether the Dinantian reservoir has similar temperature anomalies at other locations.

3.2.5 Distributed temperature sensing

Distributed temperature sensing (DTS) is a relatively novel technique that may yield temperature profiles over an entire well trajectory. This kind of temperature measurement data was not available in the database with temperature measurements prior to the start of the current study. Such data became available in the course of this study. Therefore, it will be described in the next chapter.

3.3 Dinantian and Upper Carboniferous facies types

For accurately modelling the temperature in the Dinantian, knowledge on the type and associated properties of the Dinantian rocks is required. Furthermore, the model also requires knowledge on the properties of the overlying Upper Carboniferous rocks (Namurian and Westphalian), as these may serve as an insulating layer.

The interpretation of platform vs. non-platform facies published by [Boxem et al. (2016)] was used for the previous version of the temperature model to distinguish two different facies in the Dinantian reservoir. Both are considered to have different thermal properties. The *platform* facies type was assigned a prior thermal conductivity value of 5.0 W/mK for the first steps of the temperature model workflow. This a thermal conductivity value which is higher than those published for carbonate rocks by [Hantschel & Kauerauf (2009)], of which the possible range of values is listed in Table 3.2. The specific value of 5.0 W/mK was chosen for the platform facies because a high thermal conductivity enhances the vertical heat transport, leading to an increased temperature at the top of the Dinantian. The *basin* facies type was characterised as micrite (lime mud) with a thermal conductivity of

3.0 W/mK. For the Namurian rocks the thermal conductivity was set to a value of 1.5 W/mK, corresponding to a value for a shale (Table 3.3). Hence, an insulating effect might be expected with an increase of the temperature gradient in the Namurian rocks.

Table 3.2   Thermal conductivity values of carbonate rocks, from [Hantschel & Kauerauf (2009)].

Rock class	Rock subclass	Thermal conductivity [W/mK]
Carbonate Rocks Limestone	ooid grainstone	3.0
	Waulsortian mound	3.0
	micrite	3.0
	micrite	4.5
	shaly	2.3
	org. rich typical	2.0
	org. rich 1 2% TOC	2.6
	org. rich 10% TOC	1.5
	chalk typical	2.9
	chalk 95% calcite	3.0
	chalk 75% calcite	2.7
	chalk 40% calcite	3.2
Carbonate Rocks Marl	marl	2.0
Carbonate Rocks Dolomite	typical	4.2
	organic lean sandy	4.3
	organic lean silty	3.0
	organic rich	2.2

Table 3.3   Thermal conductivity values of shale, from [Hantschel & Kauerauf (2009)].

Rock class	Rock subclass	Thermal conductivity [W/mK]
Clastic Sediments Shale	typical	1.6
		1.1
	organic lean typical	1.7
	organic lean sandy	1.8
	organic lean silty	1.8
	organic lean siliceous typical	1.9
	organic lean siliceous 95% Opal CT	1.8
	black	0.9
	organic rich typical	1.3
	organic rich 3% TOC	1.5
	organic rich 8% TOC	1.2
	organic rich 20% TOC	0.8

Table 3.4   Thermal conductivity values of sand, from [Hantschel & Kauerauf (2009)].

Rock class	Rock subclass	Thermal conductivity [W/mK]
Clastic Sediments Sandstone	typical	4.0
		3.0
	clay rich	3.4
	clay poor	6.0
	quartzite typical	6.2
	quartzite very quartz rich	6.5
	subarkose typical	4.6
	subarkose quartz rich	5.1
	subarkose clay rich	3.4
	subarkose clay poor	4.8
	subarkose dolomite rich	4.1
	arkose typical	3.2
	arkose quartz rich	4.1
	arkose quartz poor	2.0
	arkose clay rich	2.3
	arkose clay poor	4.0
	arkose dolomite rich	4.4
	wacke	2.6

3.4 Dominant heat exchange mechanism

Conduction is the dominant mechanism for (vertical) heat transport in the Dutch subsurface. Convective processes are therefore not considered in the workflow steps of the temperature model. Further background on this is provided in the remainder of this section.

Convection is a process that facilitates vertical transport of heat. It may cause a low temperature gradient within a reservoir and a higher temperature gradient in the overlying rocks. Hence, convection could be considered as a mechanism for explaining the temperature gradients measured in the LTG-01 well as is discussed in [Van Oversteeg et al. (2014); Lipsey et al. (2016)].

Whether or not conditions are favourable for thermal convection can be demonstrated by the dimensionless Rayleigh number (see [Holzbecher (1998)] and [Zhao et al. (2008)]):

$$Ra = \frac{(\rho_{f0} C_p) \rho g \alpha k \Delta}{\mu \lambda_e} \tag{3.2}$$

With:

Ra	Rayleigh number in a porous medium [-]
ρ_{f0}	fluid density [kg/m³]
c_p	specific heat of the pore fluid [J/Kg/K]
ρ	reference water density [kg/m³]
g	gravitational acceleration [m/s²]
α	coefficient of thermal expansion of the pore fluid [1/°K]
k	permeability [m²]
ΔT	temperature difference between top and bottom of the medium [°K]
H	thickness of the layer [m]
μ	viscosity of the fluid [Pa s = kg/m/s]
λ_e	conductivity of the pore fluid [W/mK]

The critical Rayleigh number Ra* is equal to $4\pi^2$ [Shiina & Hishida (2010)], [Lapwood (1948)]. The conditions for the onset of convection are favourable when the Rayleigh number is higher than this critical value. The various parameters that are required for calculating the Rayleigh number are not always known from actual measurements on rocks. Instead these can be estimated using experimental relationships found in literature. For instance, relations for the temperature dependence of density, specific heat, dynamic viscosity, thermal expansion and thermal conductivity are given in [Holzbecher (1998)]. The temperature and salinity dependence of specific heat capacity is described in [Grunberg (1970)], whereas in [Batzle & Wang, (1992)] relations between temperature, pressure and density and viscosity are provided.

The critical Rayleigh number can be used to rewrite (3.2) to become:

$$k_{min} = \frac{Ra^* \mu \lambda_e}{(\rho_{f0} c_p) \rho g \alpha k \Delta T H} \tag{3.3}$$

This equation yields the minimum required permeability k_{min} for the onset of thermal convection. Assuming a layer thickness of 700 metres (which is approximately the thickness in the LTG-01 and UHM-02 wells) and an average thermal gradient of ~0.031 °C/m, the average permeability required for convection to occur is in the order of tens to hundreds of mD. Even if a high thermal gradient or low viscosity are assumed, the required permeability is still high. In [Van Oversteeg et al. (2014)] it is concluded, on basis of interpretations of evidence from the LTG-01 well like core plug data and RFT tests, that the average permeability may be in the order of tens of mD. In [Lipsey et al. (2016)] it is shown that, when a sufficiently high permeability is assumed, convection of hot reservoir fluid may start, resulting in the observed very steep temperature gradient in the Dinantian rocks as shown in Figure 3.7. From this figure it should be noted that at iso-depth levels, temperatures difference up to about 20 °C may exist.
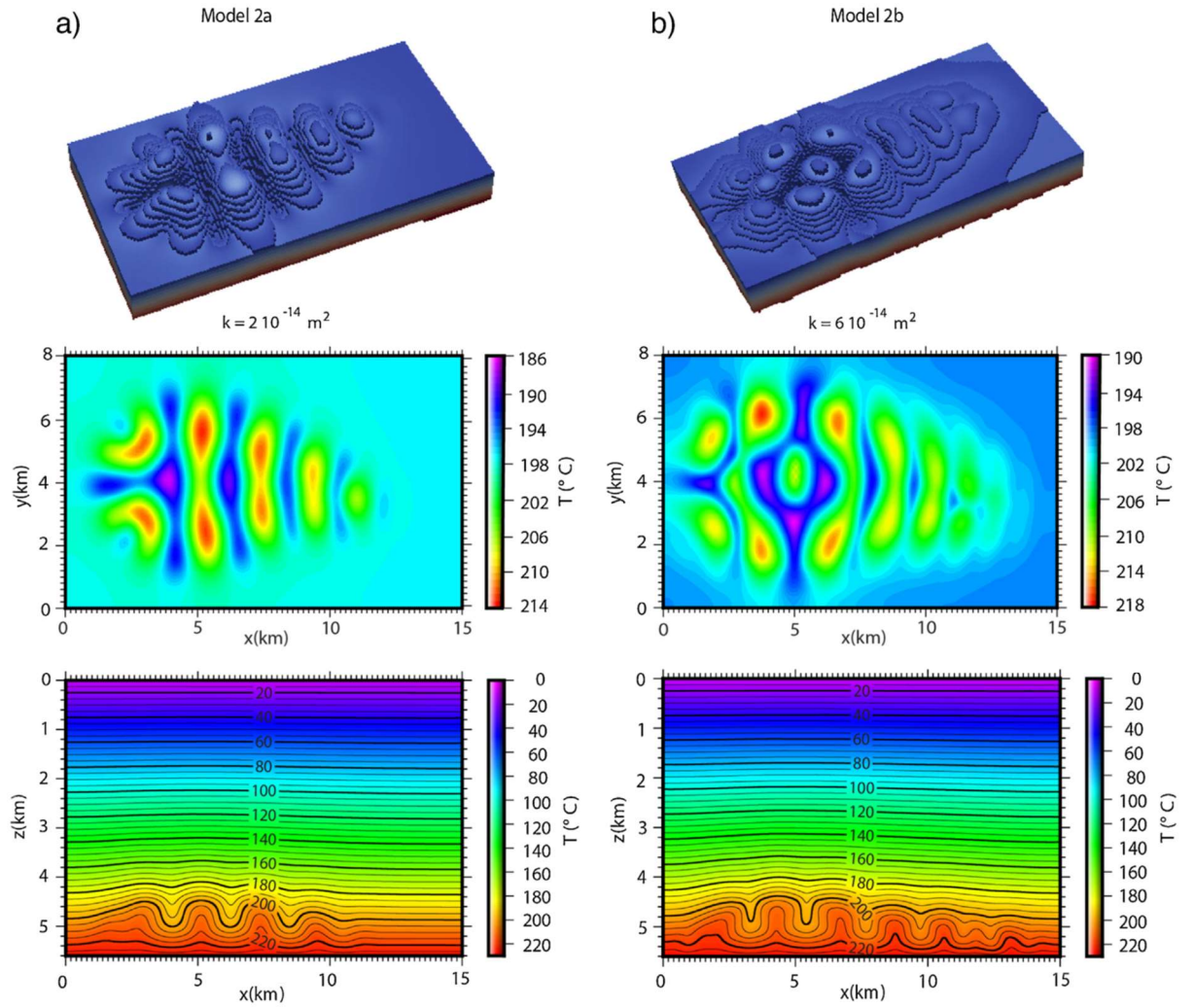
Figure 3.7   Modelled temperature distribution in a carbonate platform modelled after Luttelgeest for permeabilities 20 and 60 mD (from [Lipsey et al. (2016)]).

At the start of the study subject of this report, the opinions on the likelihood of convection as a driving mechanism were such that this could be a possible explanation (given sufficiently high permeability) of the observed temperature gradient. Until then this observed temperature behaviour in the Dinantian rocks was modelled by assuming values of the thermal conductivity that are slightly anomalous in view of the tables in [Hantschel & Kauerauf (2009)], i.e. the values provided in the previous section of this chapter.

Whether or not convection is a relevant process for the modelling of temperature in the Dinantian rocks depends on numerous assumptions. Other SCAN studies, such as on petrophysics [Carlson (2019)], on facies distribution and diagenesis [Mozafari et al. (2019)] and on fractures [Van Leverink & Geel (2019)] could be used to further consider whether convection is likely or not a dominant mechanism in the Dinantian rocks.

4 Enhanced temperature model: additional data and modelling

In order to accomplish an enhanced temperature model (e.g. to provide a better estimate of the temperature distribution in the Dinantian) various new data sources were studied and added in this project. The most important ones are described in the next sections and concern:

- Additional temperature measurement data;
- Revision of the distribution of Dinantian facies and their corresponding reservoir properties;
- New structure maps of Carboniferous layers, and of Permian through Tertiary layers.

Via the workflow steps of the enhanced temperature model, a temperature distribution has been obtained for the Dutch subsurface. This will be discussed for the Dinantian in Chapter 5.

4.1 Additional temperature data

For the enhancement of the temperature model several new temperature data sources, as listed in Table 4.1, were added to the database with temperature measurements. These sources are described in the remainder of this section.

Table 4.1   New temperature data available for the updated temperature model

Source	number of measurements	remark
SCAN Horner corrected data, [Carlson (2019)]	26	medium accuracy
Temperature monitoring [Clemens Visser, pers. comm.)	56	high accuracy
Zeerijp-3 fibre optic [Cannon & Kole (2018)],	16	1-metre vertical resolution, 0 - 3239 mTVD, resampled to 200 m vertical model resolution
NAM GFR temperature map ([Burkitov et al. (2016)]	67	low accuracy

4.1.1 Horner corrected data

The most important new source of data consists of subsurface temperature measurements that were Horner corrected within the SCAN study reported in [Carlson (2019)]. The dataset comprises 26 temperature estimates in eight wells at depths between 467 and 5100 metres below surface (mTVD). Of those 26, 6 pairs of temperature estimates originate from the same well and at the same depth. For instance, for the well KTG-01 temperature estimates of 71.3 and 71.6 °C were made at a depth of 1875 mTVD. Those pairs of estimates were calculated using different combinations of the raw data, usually by excluding observations that may be considered unreliable. For the KTG-01 example, the second temperature was

calculated using 3 of 4 (time,Temperature) observations. All graphs in [Carlson (2019)] show the graphical Horner correction solution for circulation times fixed to values of one, two and four hours, because exact circulation times are rarely found in the raw data.

Figure 4.1 shows the application of the Horner correction graphically for one of the Luttelgeest BHT measurements. On the horizontal axis time increases to the left (infinite time at x=0), so the equilibrium temperature is slightly over 191 °C. It becomes immediately clear that the predicted equilibrium temperature becomes unreliable when the time between the first and last measurements is small and the difference between the measures temperatures and the equilibrium temperature is large. This measurement fulfils the criteria defined by [Peters & Nelson, (2009)] for a reliable temperature estimate. When such criteria are applied to all 26 Horner corrected temperatures, 10 meet all three criteria, 11 meet two of the three criteria, and five meet only one of the criteria (mainly because only two data points were used). When the rule, as defined in [Shen & Beck, (1986)], that the condition (3.1) should be avoided, only the measurements in the Geverik well and one measurement for well O18-01 should be discarded when assuming acceptable values for the thermal diffusivity (e.g., between 0.5 m^2/s and 2.0 m^2/s according to [Fuchs, (2018)]). For those wells, [Carlson (2019)] lists a time since circulation in minutes which is very small. This may be questionable. However, the majority of the measurements has a dimensionless value around 0.06 when a diffusivity of 1 m^2/s is assumed which is way below the threshold of 1 explained in equation (3.1).

4.1.1.1 Comparison between Horner corrected temperatures

As discussed in the previous chapter, most BHT data are not equilibrium and must be corrected to better reflect the reservoir temperature. Because of their abundance, the temperature correction (ICS and AAPG) is computer coded and applied in an automated fashion. The Horner temperature correction performed in [Carlson (2019)] was done manually using linear regression. A comparison between the BHT and Horner corrected temperature data is possible, although it should be noted that for the Horner correction at least two or (better) three suitable measurements (at comparable depths but different recording times) are required, whereas in the temperature model database with temperature measurements also single measurements are stored. These latter ones cannot be corrected for nonequilibrium and therefore have a large associated error. Figure 4.2 shows the Horner corrected temperature data and those currently available in the model database. The chart also shows the Horner corrected temperature data of the LTG-01 well that were used in [Van Oversteeg et al. (2014)]. The latter data corresponds well to the data of [Carlson (2019)]. There is only a small vertical offset probably caused by a different interpretation of the exact depth, or the AH-TVD conversion. The automatically Horner corrected data in the model database with temperature measurements appear to be underestimating the Horner temperatures for the LTG-01 and WSK-01 wells. For the other corresponding wells, KTG-01 and GVK-01, the temperatures correspond well.

4.1.1.2 Horner corrected temperatures versus temperature gradient

With respect to the temperature gradient that is often used as an average for the Netherlands, the deeper measurements (3000 metre and deeper) all fall above this gradient (KTG-01, WSK-01, LTG-01, UHM-01, S02-02, Figure 4.2), about 10–20 °C for the WSK-01 well and 20–40 °C for the LTG-01 well. On the other hand, *within* the Dinantian in LTG-01, the temperature gradient appears to be low according to the Horner temperatures. On the basis of the Horner corrected data there is a general tendency for the temperature in the Dinantian to be higher than expected from the average Dutch temperature gradient (Figure 4.2). Therefore, in order to reach the observed high temperature *in* the Dinantian, the temperature gradient needs to be steep *above* the Dinantian, i.e., in the Upper Carboniferous and above.

As already mentioned in section 3.4, the question that needs to be addressed is what causes this deviation from the average temperature gradient, and whether it can be expected in parts of the Dinantian reservoir for which no measured temperature data are available. Options are: higher heat flow, authigenic heat production, thermal convection (for which a relatively high permeability is required), or different thermal conductivity values than previously assumed (both in and above the Dinantian rocks). Alternatively, the average gradient may not be valid because it is based on data that may be biased towards lower temperatures.
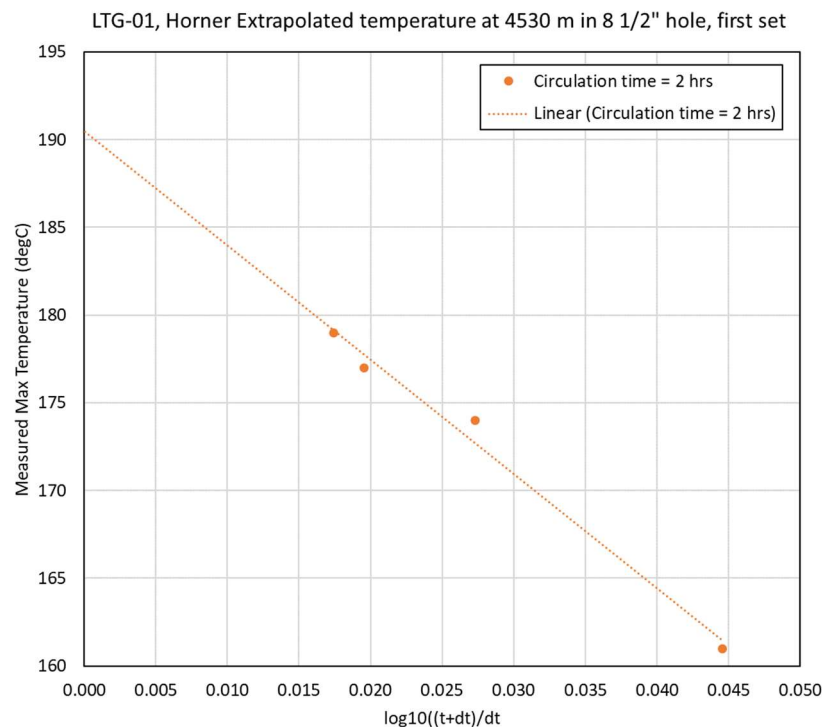
Figure 4.1   Horner correction on one of the LTG-01 BHT measurements.
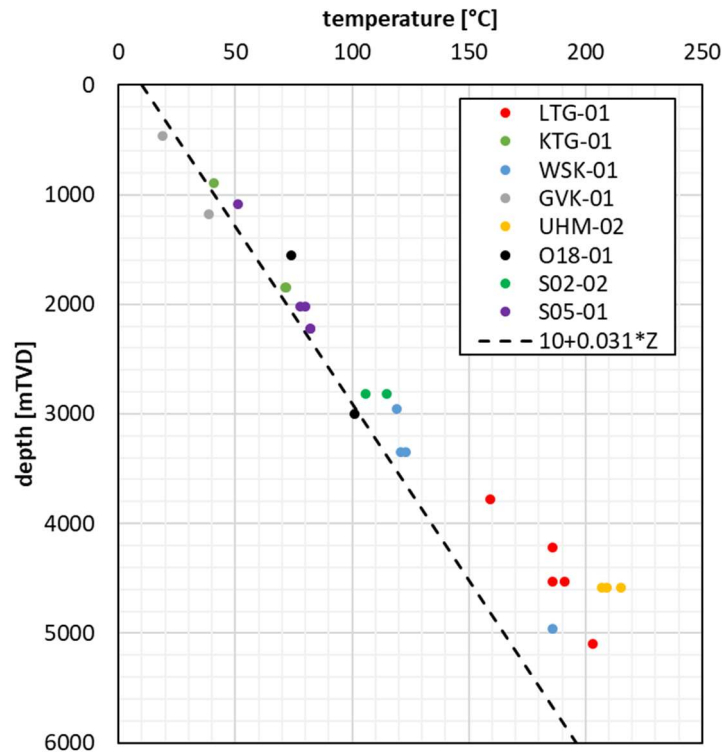
Figure 4.2   Horner corrected temperature measurements by [Carlson (2019). Dotted line: assumed average Dutch temperature gradient.

4.1.2   Groningen area temperature data

Another source of temperature data concerns a dataset within the Groningen area available from NAM, partly through public research reports published on www.nam.nl, under 'feiten en cijfers', partly on special request. Most of this data is measured or monitored at or around top Rotliegend level. This data is relevant for the temperature at Dinantian level because the temperature at Rotliegend level is also indicative of deeper temperatures, since a high temperature in deeper strata generally leads to heating of shallower strata. The exact nature of the correlation is steered by the thermal conductivity of the layers. A low thermal conductivity (isolation, like in shales) leads to a high temperature gradient, whereas a high thermal conductivity (like in salt) leads to a low gradient. The proximity to the Dinantian carbonate platforms Uithuizermeeden and Friesland, and the accuracy of the (equilibrium) data, makes this dataset a valuable addition to the database of temperature measurements. A comparison of this dataset with the temperature distribution obtained with the prior (2018) version of the temperature model (as described in [Békési et al. (in prep.)] showed that the dataset provides higher temperatures than previously modelled (Figure 4.3, Figure 4.5). In [Burkitov et al. (2016)] the temperature anomalies are attributed to differences in Zechstein thickness. For the prior (2018) temperature model, few temperature measurements were available in the Groningen area. The difference between the two temperature maps shown in Figure 4.3 is, on average, 6 °C. The temperature distribution is remarkably similar for both maps because it is dominated by the depth structure of the top Rotliegend which is well constrained. Therefore, local temperature anomalies that do not result from differences in the

depth of the Rotliegend are obscured in Figure 4.3. The temperature map at a constant depth of 2800 metres, shown in Figure 4.4, however, also shows a similar structure with relatively high temperatures in the Northwest – located in between the Friesland and Uithuizermeeden platforms, and the Southeast.

The Groningen area temperature dataset consists of the following items:

- Temperature monitoring time series for a set of wells
- Zeerijp-3 distributed temperature sensing
- Near top reservoir temperatures.

This data is further discussed in the remainder of this paragraph.

4.1.2.1 Temperature monitoring time series

Monitoring data originating from 56 gas wells which are located either over or very near to the Groningen gas field or at Geesbrug, Blija-Ferwerderadeel and Ameland Westgat is part of the dataset obtained. In these 56 wells the bottomhole temperature is being or has been monitored for shorter or longer periods, between 1965 and 2008. These monitored temperatures were extrapolated to a datum level of 2875 mTVD which roughly coincides to the top of the Rotliegend. For this data it has been confirmed that the temperature data has been determined from SPTG (Static Pressure and Temperature Gradient) measurements over longer periods [Burkitov et al. (2016)], and furthermore that the temperatures approach equilibrium with the specific reservoir temperatures [Clemens Visser pers. comm.]. The presence of the well could affect this equilibrium as heat transport along the casing may occur and the next paragraph discusses this in more detail. Furthermore, it is not known if the monitored temperatures are corrected for the Joule-Thomson effect. This effect describes the cooling caused by expansion of a real gas or liquid when it is produced in a well through a perforation (assuming the expanding gas is insulated so there is no heat exchange with the environment). The magnitude of this effect depends on gas type, temperature and pressure. For methane at 100 °C and 200 bar it is 0.13 °C/bar. This means that at these conditions a pressure drop of 10 bar results in a temperature decreased of 1.3 °C (analysis based on NIST Chemistry Webbook[4]). However, 21 of the 56 wells are observation wells, where the Joule-Thomson effect does not play a role. The remaining 35 wells are currently either producing, abandoned, suspended or closed in. The average temperature of the observation wells at datum level is 104.0 °C. For all other wells it is 99.6 °C, which suggests that the Joule-Thomson effect plays a role and that the temperatures from those wells needs to be corrected in order to be used. This was not done in the current study and the measurements were used 'as is'.

---

[4] webbook.nist.gov/chemistry/fluid/ (thermophysical properties of fluid systems), accessed on February 28th 2020
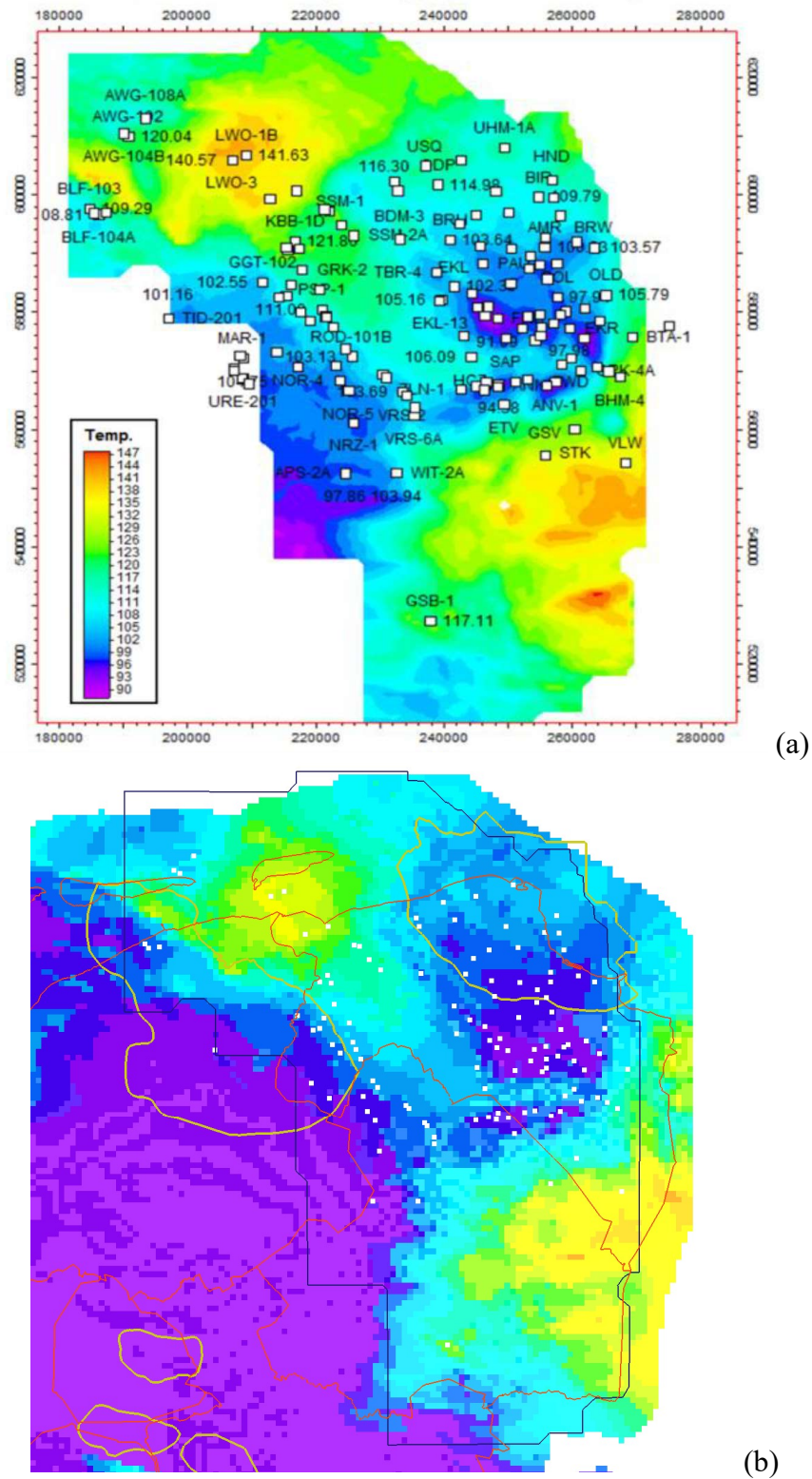
Figure 4.3   Comparison between top Rotliegend temperature (a) published in
               ([Burkitov et al. (2016)] and top Rotliegend temperature distribution from
               the prior (2018) temperature model (b). Outlines of the Uithuizermeeden
               and Friesland platforms and the [Burkitov et al. (2016)] model overlain.
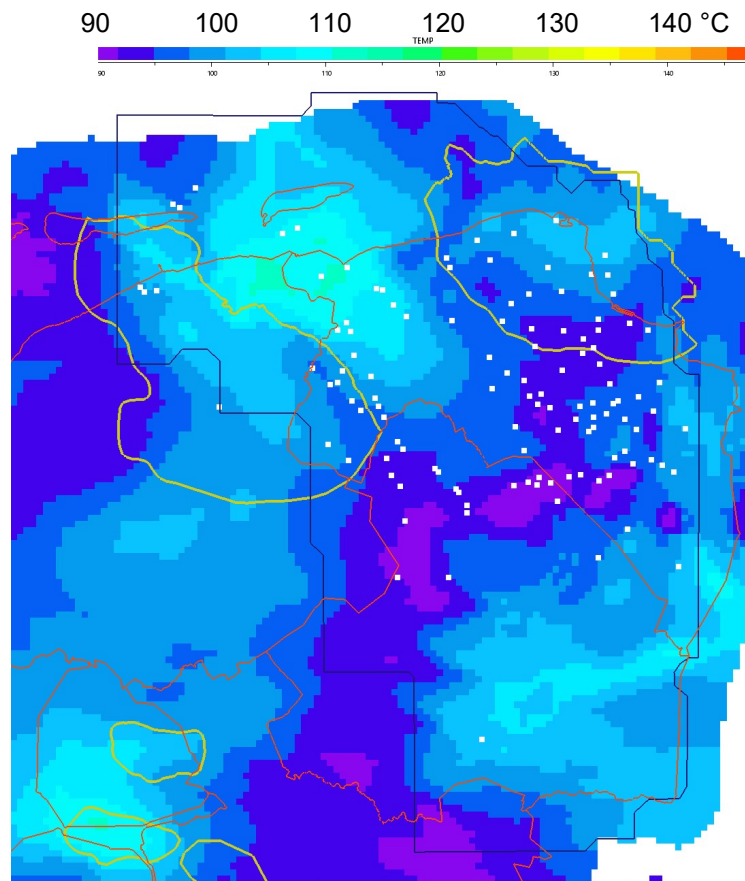
Figure 4.4   Temperatures at 2800 metres depth obtained with prior (2018) temperature model.
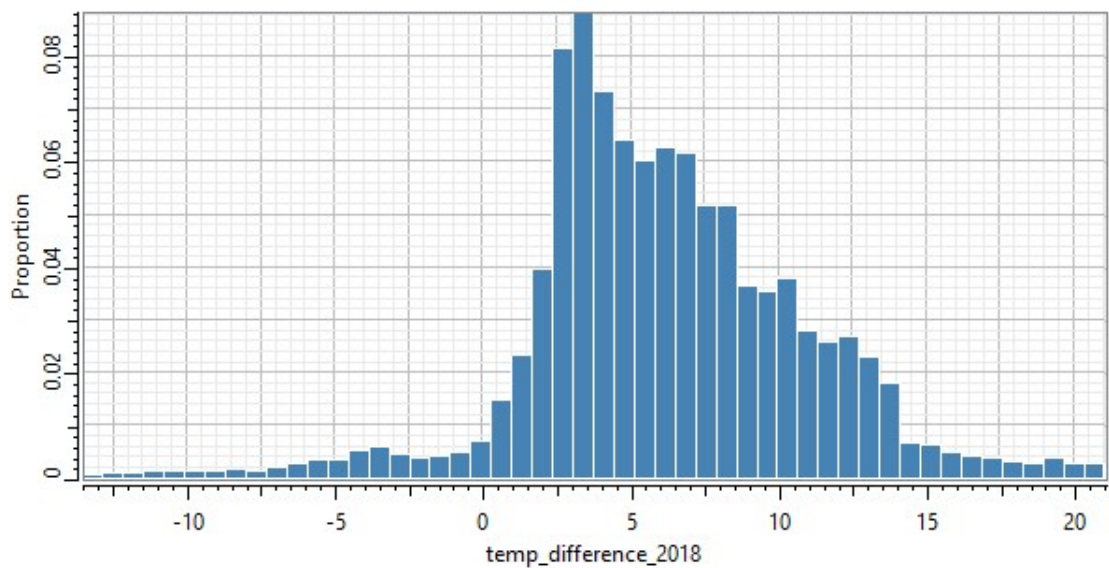
Figure 4.5   Difference between the NAM Groningen temperature map @2875 mTVD, from [De Jager & Visser, (2017)], and the prior (2018) temperature model.

This monitoring data only partly coincides with the wells shown in Figure 3.3 that were used to generate the top Rotliegend temperature map shown as bottom display in Figure 4.3. For each well at least one, but more often multiple measurements are available. Figure 4.6 shows that the temperatures within a single well are indeed relatively constant, but exhibit variations of around ±2 °C, which is also the uncertainty assigned to the measurements reported in [Burkitov et al. (2016)]. Specific trends in the variations are not observed. The cause of these variations is unknown but may be due to measurement or sensor inaccuracy.
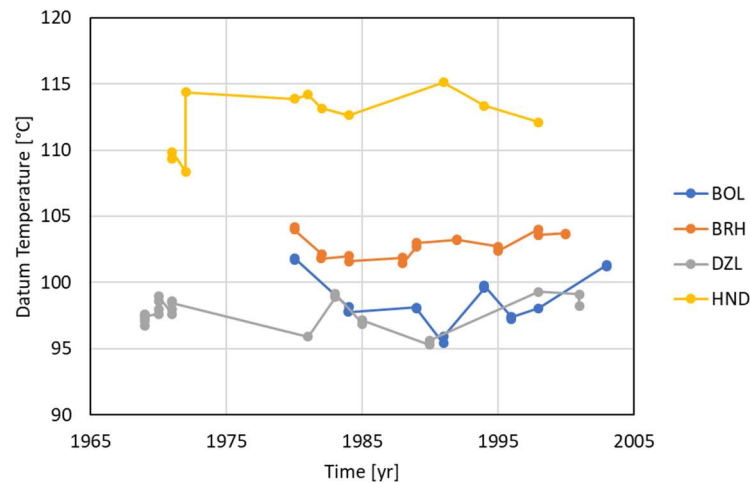
Figure 4.6   Temperature profiles of 4 observation wells from the NAM dataset at 2875 mTVD reference level. BOL = Bolderij, BRH = Barnheem, DZL = Delfzijl, HND = De Hond.
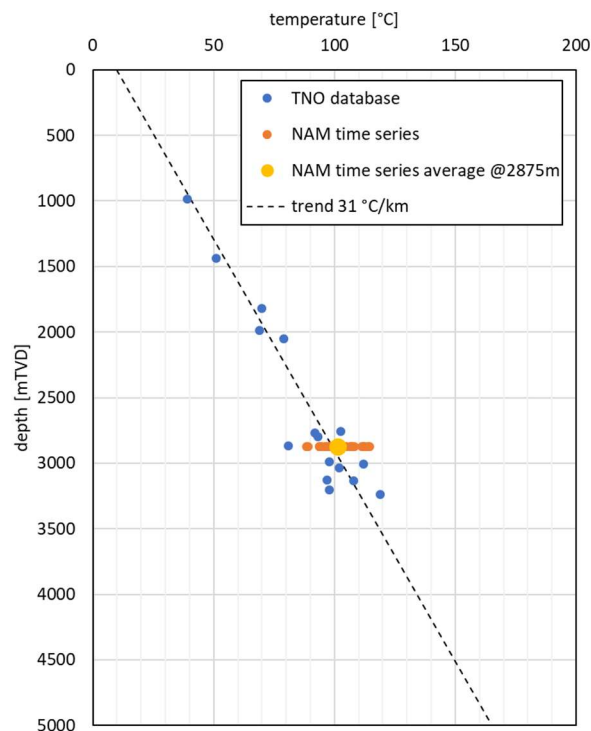
Figure 4.7   Comparison between the model database with temperature measurements in the Groningen area and the NAM time series data @2875mTVD, for the corresponding wells.

40

This monitoring dataset is reasonably well in line with the database with temperature measurements of the prior (2018) temperature model, as can be observed in Figure 4.7. Only a few wells (Annerveen-Veendam-01, Delfzijl-01, De Hond-01, Nieuw Roden-01, Ten Boer-01 and Uithuizermeeden-02) were already in this database. At datum depth, the difference with the model database is a few degrees, whereas the difference between the temperature obtained from the commonly used gradient (i.e. 10 + 0.031*Z) and the average of the time series is small.

4.1.2.2 Zeerijp-3 distributed temperature sensing

Distributed temperature sensing (DTS) is a relatively novel technique explained in [Ukil et al. (2012))]. It uses fibre optic cables to measure the temperature along a (vertical) profile, often in but not restricted to boreholes. In the publications of [Cannon & Kole (2018)], [Lee et al. (2018)] and [Balling et al. (2016)] it is shown that this kind of data is very valuable for obtaining subsurface temperature estimates. The fibre optic cables often remain in the borehole for long periods of time. Sometimes they are even installed behind the casing. Therefore, equilibrium temperatures can be measured using this technique. Like measurements from geothermal wells, fibre optic measurements have a high accuracy; [Ukil et al. (2012)] found the accuracy to be in the order of ±1 °C In the publications of [Cannon & Kole (2018)], and [Lee et al. (2018)] it is emphasized that DTS measurements can be disturbed by changes in temperature of the interrogator and by defective sensors in the well, and that it may take several months before the temperature reaches equilibrium after drilling operations. Although the installation of a steel casing in the subsurface disturbs the virgin reservoir, and the thermal conductivity of steel is about 20 times higher than of common rock types (thereby enhancing heat transport to the shallow subsurface), the thermal effect of the casing is limited. This is because the specific volume of the casing is relative very small (in comparison with the surrounding reservoir layers) to accommodate a significant disturbance (via large heat flows) of the reservoir temperature near the well bore. This limited thermal effect of the casing has been studied via a few steady state heat conduction calculations for a characteristic representative setting and which are described in Appendix C. In a similar way it is expected that an analysis of convectional flow in the wellbore due to temperature and density differences will reveal that the heat exchange as a consequence will not introduce a relative high difference between well bore temperature and reservoir temperature.

High resolution fibre optic Distributed Temperature Sensing (DTS) data for the Zeerijp-3 observation well, located about 20 kilometre North-East of Groningen has been obtained for this study. The well was drilled between May and July 2015. The temperature data was obtained between October 2015 and October 2016. The data is shown graphically in Figure 4.8 and also discussed in [Cannon & Kole (2018)]. From this report it becomes clear that temperature equilibrium was obtained several months after observation started.

The monitoring dataset as provided by NAM has a vertical resolution of 1 metre. It has been resampled for the modelling purposes our study to the vertical resolution of 200 metre of the 3D model grid as used in step 5-8 in the workflow of the temperature model. Apart from the DTS data, [Cannon & Kole (2018)] also contains the results of a Horner corrected data point near the total depth of the well in rocks of Carboniferous age. At top Carboniferous level the difference between the DTS data and the temperature distribution obtained with the prior (2018) temperature model (for which no temperature data around Zeerijp was used) is about 20 °C, whereas for the Horner corrected temperature point at 3200 metre depth this difference is even more. Similar to the monitoring time series data described above, the Zeerijp temperature dataset has a gradient exceeding 0.031 °C/m. A notable feature is the relatively low increase in temperature between 0 and 500 metres depth. Various factors, or a combination of two or more, may be responsible for this gradient. A description of these factors is given in section 5.1.
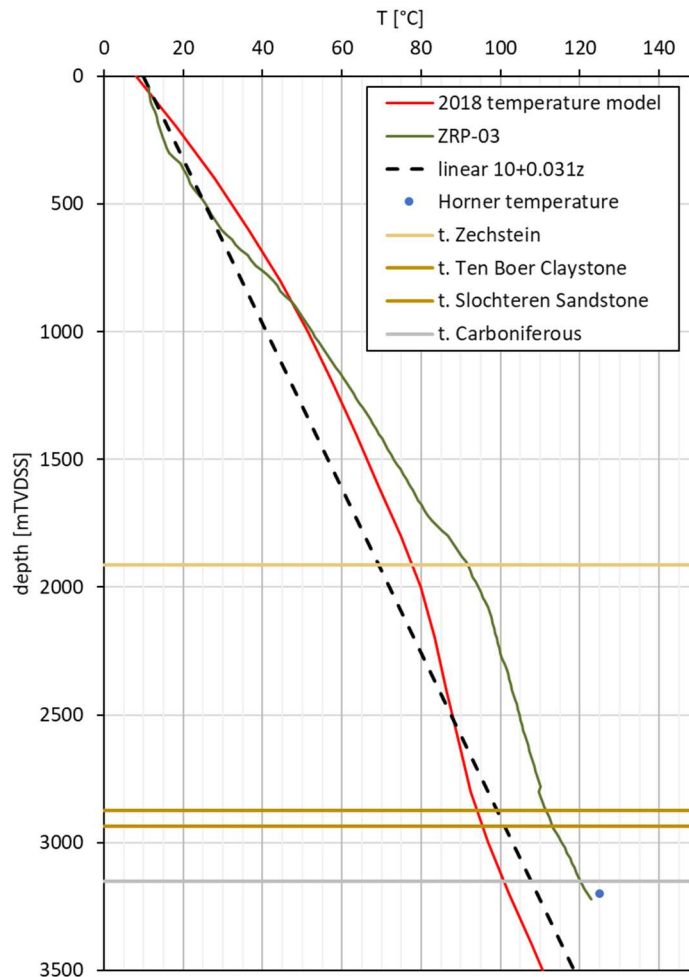
Figure 4.8   Comparison between temperatures obtained with the prior (2018) temperature model (red), generated without the new Groningen area measurement data, and the Zeerijp-3 DTS data (green). Linear gradient (black) for reference.

4.1.2.3 Near top reservoir temperature

A further 87 datapoints were obtained for the additional data source via digitization of the near top reservoir temperature map of the Groningen field at a depth of 2875 metre, available in [Burkitov et al. (2016)] and shown in Figure 4.3 (a). Twenty of these points overlap with the temperature monitoring data described in paragraph 4.1.2.1 and were therefore discarded. The remaining 67 datapoints have a lower accuracy because they have been digitized from a map, and the temperature extraction from the colour coding in the map. In order to estimate the accuracy of these datapoints, a comparison has been made with the between the 20 discarded points and the temperature monitoring data. Figure 4.9 shows that the accuracy is about ±5 °C.
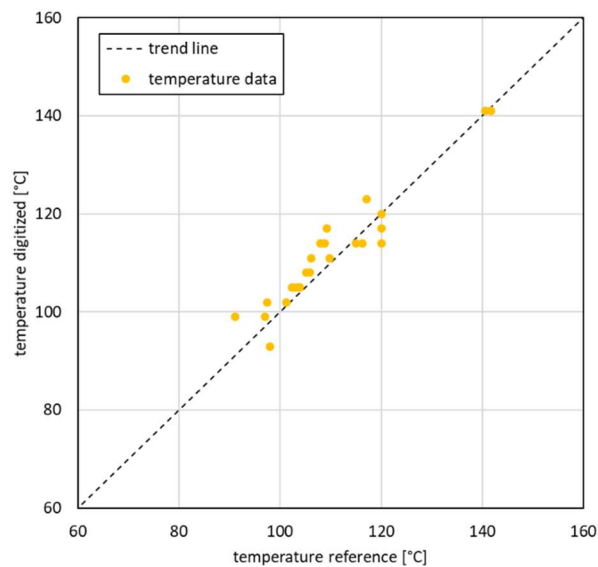
Figure 4.9   Comparison between temperature monitoring reference data (horizontal axis) and digitized near top reservoir temperature (vertical axis).

4.2 Improved estimations of rock properties

This section discusses some of the results of the SCAN studies petrophysical analysis reported in [Carlson (2019)], and fracture characterization of the Dinantian rocks reported in [Van Leverink & Geel (2019)]. The goal is to improve the assignment of rock properties to the Dinantian, Namurian and Westphalian rocks in the temperature model in order to arrive at a sufficiently accurate temperature distribution for the Dutch subsurface, and specifically the Dinantian. To this end, detailed knowledge of thermal properties is a key issue ([Fuchs, (2018)]).

4.2.1 Permeability

For various studied wells, an estimate of the porosity of the Dinantian carbonates was made. With the exception of short intervals occurring in all wells, the porosity is in the order of 1-2% or even less [Carlson (2019)]. This is illustrated by the well panels for LTG-01 and UHM-02 found in in Appendix A. The only intervals with

elevated porosity are the ones that were dolomitized or fractured / karstified. Here, the maximum porosity reaches 10% at most in limited intervals and even up to 25-32% in very thin intervals.

The permeability could not be determined due to the very low porosity. Only a small number of permeability measurements from cores are available, and the permeability was found to be lower than the detection limit [Carlson (2019)]. The permeability in the low porosity ranges is probably in the order of micro-Darcies. In the high porosity ranges occurring in fractured and karstified zones, the permeability could be orders of magnitude higher.

In [Van Leverink & Geel (2019)] the FMI (Formation Micro Imager) logs of the LTG-01 and CAL-GT-01 wells were analysed. These analyses show that, although the reservoirs in these two wells contain abundant fractures, the secondary permeability is insufficient to produce significant amounts of fluid. Exceptions are the CAL-GT-01, CAL-GT-03 and CAL-GT-04 wells that rely on the permeability caused by the presence of the Tegelen fault zone. Outside the fault zone, fractures are also present (as proved by the FMI) but they do not offer sufficient permeability for a sustainable flow rate.

Regarding the interpretation of RFT-tests by [Van Oversteeg et al. (2014)], it is concluded in [Van Leverink & Geel (2019)] that the deduction of high permeabilities from those tests was based on an erroneous assumption of the fluid viscosity. The resulting permeabilities are therefore lower by a factor of about 100.

From the above, together with the outcome of section 3.4, it can be concluded from abundant evidence that it is very unlikely that the primary and secondary porosity and permeability are able to support significant convection. This also means that the conductive approach that was until now followed for the temperature model is also valid for the Dinantian rocks. Another mechanism is therefore responsible for the observed temperature anomalies in, especially, LTG-01 and WSK-01. Possibly other thermal properties like thermal conductivity, discussed in the next paragraph, can be the cause.

4.2.2 Thermal conductivity

The observations on the temperature gradient in the Upper Carboniferous (high) and Dinantian (low) rocks suggest that the relevant rock properties differ from the 'average' rock properties observed in younger strata, which lead to a gradient of approximately 0.031 °C/m according to [Bonté et al. (2012)].

In the temperature model, rock properties are assigned to the various layers using the thermal properties published by [Hantschel & Kauerauf (2009)]. In order to calculate the bulk rock thermal conductivity, the porosity needs to be estimated to correct for the lower thermal conductivity of the pore fluid (although this is less relevant for tight rocks such as the Dinantian).

Given the fact that the Dinantian mostly consists of limestone and dolomite, and is overlain by (mostly) Namurian (and Westphalian) shale, the following lithologies require attention:

- For shales, [Hantschel & Kauerauf (2009)] suggest values between 0.8 and 1.9 W/mK (Table 3.3).
- Limestone has thermal conductivities between 1.5 and 4.5 W/mK (Table 3.2).
- Dolomite varies between 2.2 and 4.3 W/mK (Table 3.2).

The layers modelled in the 3D grid on basis of the latest geological model DGM-Deep v5 (see also the next section) are heterogeneous on a regional and national scale, which concerns tens to hundreds of kilometres. Their conductivities will vary laterally according to their specific lithological composition. Therefore, in the temperature model average lithological compositions are given for all layers in terms of percentages of the contributing lithologies. From this composition, bulk thermal conductivities are calculated, considering porosity-depth relationships. The initially calculated bulk thermal conductivities will then be adapted, allowing for spatial variation, via inversion in the workflow steps 4 and 8 as explained in chapter 2. Because little is known about the (variations in the) lithological composition of the Namurian/Westphalian and Dinantian rocks, average values of 1.5 and 5.0 W/mK were adopted in previous model runs, respectively. For shale this is an average value, whereas for limestone and dolomite the value is high when considering [Hantschel & Kauerauf (2009)]. This relatively high value was adopted to be able to reproduce the temperature gradients in the Namurian/Westphalian vs. the Dinantian, which was previously assumed to be caused by convection by [Lipsey et al. (2016)]. For the (unknown) Dinantian outside the platforms, lime micrite (mudstone) was adopted, having a thermal conductivity of 3.0 W/mK.

In order to obtain better initial values of the actual thermal conductivity values of the rocks in the Dinantian) and Namurian/Westphalian rocks, several 1D temperature models were constructed, similar to the temperature model workflow steps 1 and 5. A lithological succession representative of the LTG-01 well was adopted (Figure 4.10), using the stratigraphy from this well, the varying thermal conductivity values taken from the prior (2018) temperature model, and previously established assumptions for the heat flow. The thermal conductivity values were then varied in order to reproduce the measured temperature profile of the LTG-01 well. Figure 4.11 shows the results.

This variation of conductivity values was done in the following way: first, the thermal conductivity of the Namurian shale was fixed at an average value of 1.5 W/mK. The values within the Dinantian were then changed between 2 and 5 W/mK. These are low and high values, respectively, for the relevant rock type, the value of 2 being representative for organic rich limestone and the value of 5 for organic lean dolomite (see Table 3.2). In Figure 4.11 the orange and red curves show that a high thermal conductivity increases the temperature gradient in the Namurian (curves shift to the right), but that the observed temperature of the LTG-01 well cannot be

reproduced. If, on the other hand, the thermal conductivity of the Namurian shales is varied between 0.7 W/mK and 1.25 W/mK, and an average value of 3.5 W/mK is used for the Dinantian, the gradient drastically changes. The blue curves show that in the Namurian the gradient is increased, and the measured temperatures can be reproduced when a value of 0.9 W/mK is used. In [Hantschel & Kauerauf (2009)], on the other hand, values lower than 1 W/mK are suggested only for organic rich and black shales and other types of shale have values between 1.1 and 1.9 W/mK. Unpublished TNO results on 18 samples from the LTG-01 well show that the average total carbon (TC) within the Namurian is about 3.5%, which would give a thermal conductivity of about 1.5 W/mK according to [Hantschel & Kauerauf (2009)]. It should be noted though that the thermal conductivity values presented in [Hantschel & Kauerauf (2009)] are not literature referenced and, therefore, it cannot be checked if these were measured in relevant rocks.

As a further step, therefore, these presented values were compared to values found in literature. Figure 4.12 shows the results. The lithological composition of the Upper Carboniferous in the LTG-01 well was adopted from the litholog shown in Figure 4.10. This figure shows that the dominant lithology is shale, with significant amounts of silt and sand, and some coal and intrusive. Using this composition and reference values found in [Hantschel & Kauerauf (2009)], the observed thermal gradient cannot be reproduced. For limestone and dolomite there is a strong tendency for the thermal conductivity to decrease with increasing temperature. At a temperature of about 200 °C (LTG-01 at Dinantian level), dolomite is around 4 W/mK, whereas limestone / calcite is roughly between 1 and 3 W/mK. On the other hand, where in [Hantschel & Kauerauf (2009)] the values for limestone are between 0.7 and 1.9 W/mK, various other authors report values that are around, or often slightly below, 1 W/mK. This would be in good agreement with the results with 1D temperature modelling.

The Upper Carboniferous (Westphalian) is sometimes assumed to contain more sand (higher thermal conductivity, see Figure 2.1), but also more coal (which has a lower thermal conductivity). Based on the litholog of LTG-01 alone, it may be argued that on average the amount of sand in both the Westphalian and the Namurian is more or less the same, and that the resulting thermal conductivity is low for both. This could then mean that the observed temperature gradient can be explained by assuming a thermal conductivity for the entire Upper Carboniferous that is higher than 0.9 W/mK. When a conductivity value of 1.1 W/mK is adopted for both layers, a good fit between measures and modelled temperature can also be obtained. This fit does not require the very steep gradient which is the result from the thermal conductivity value of 0.9 W/mK for the Namurian only. Instead, the resulting gradient is gentler throughout the Westphalian and Namurian, resulting in the same high temperature in the Dinantian, and honouring the temperature measurement in the Namurian. It should be noted however that the lateral lithological variation within the Westphalian and Namurian is large, and that the shale content (and resulting insulating nature) may be different at other locations.
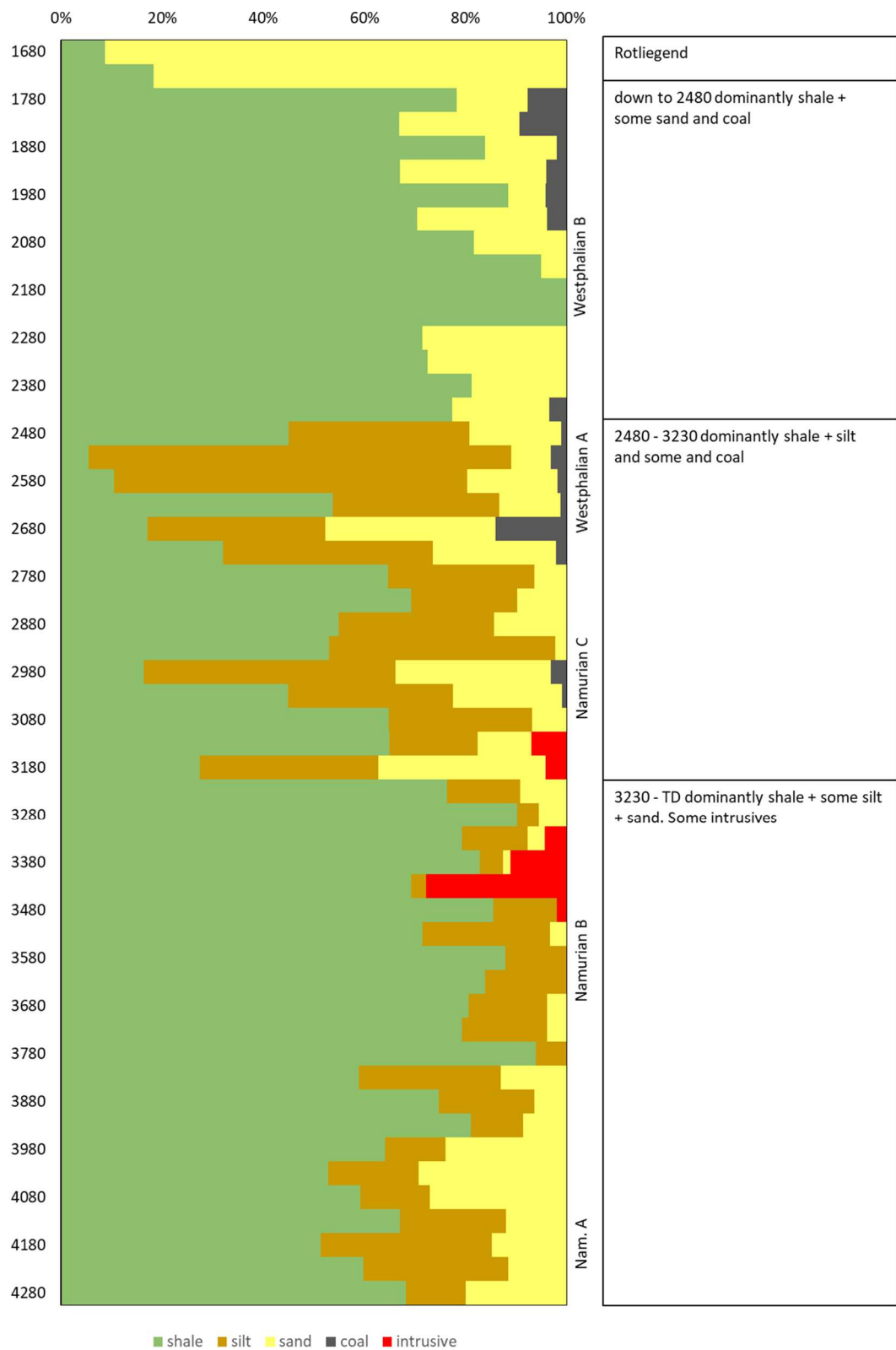
Figure 4.10   Lithological composition of the Carboniferous section of the LTG-01 well based on the litholog.
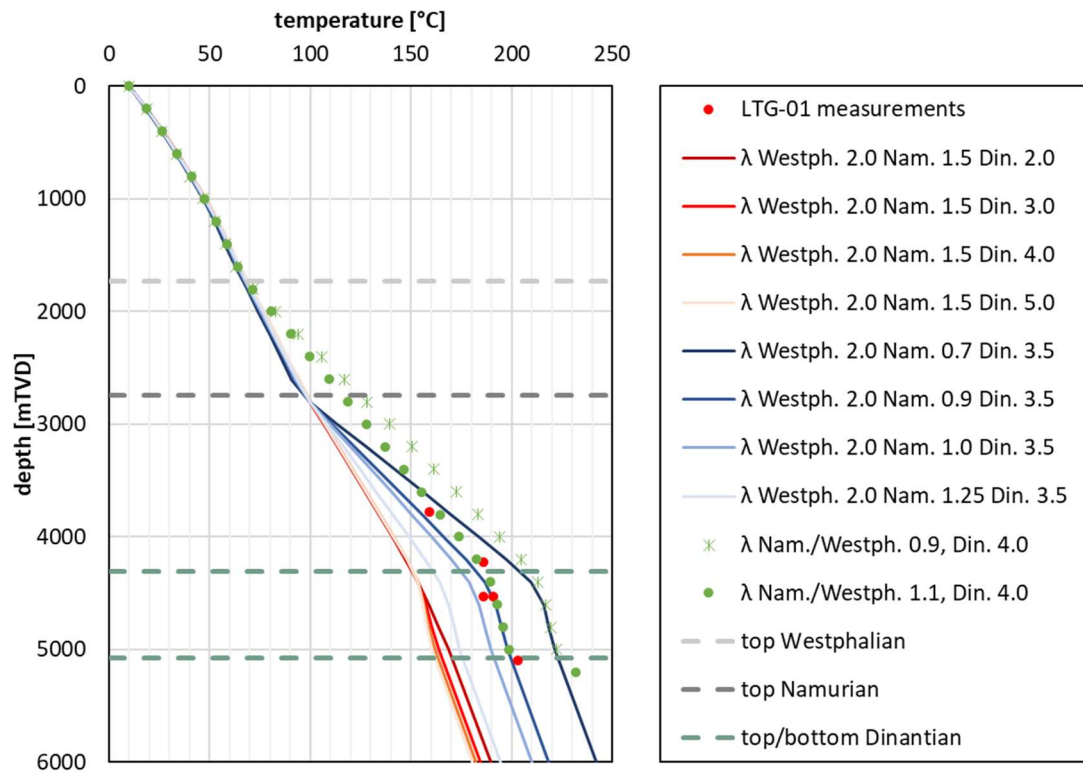
Figure 4.11   Temperature profiles from 1D modelling for LTG-01 for various thermal conductivity values for Namurian (Geul) and Dinantian (Zeeland).

Assumptions regarding the net-to-gross ratio for the Namurian and Westphalian is speculative as long as not more data becomes available. Also, the fact that only a single, possibly uncertain, Horner temperature measurement is available to determine the temperature gradient in the Namurian makes the estimation of suitable thermal conductivity values for the Upper Carboniferous speculative.

The optimal value of the thermal conductivity for the basinal equivalent of the platform rocks is largely unknown. The rocks were drilled only in the Winterswijk well, which is located just south of a presumed platform, making it possibly less representative for the 'average' basin facies. In this well only four Horner corrected temperatures are available (see Figure 4.2). These were measured at depths that make it difficult to check any hypothesis regarding the thermal conductivity values for the Namurian (and Westphalian).

For the enhanced (3D) temperature model it was decided to adopt a value of 1.1 W/mK as initial value for the Westphalian and Namurian rocks, and 4.0 W/mK for the Dinantian platform carbonates. These values are not necessarily the optimal values for the entire country, but the inversion procedure (workflow steps 4 and 8, see chapter 2) allows such initial values to be changed within specified limits in order to obtain a better model fit with temperature measurement data.

48

Figure 4.12   Relations between temperature and thermal conductivity for limestones and shale.

4.3 Further geological modelling

In the previous chapter it was explained that for the prior (2018) temperature model the representation of the Dinantian in the 3D grid was simplified because of the lack of accurate depth and thickness data, whereas the younger layers were adopted from the DGM-Deep v4 model.
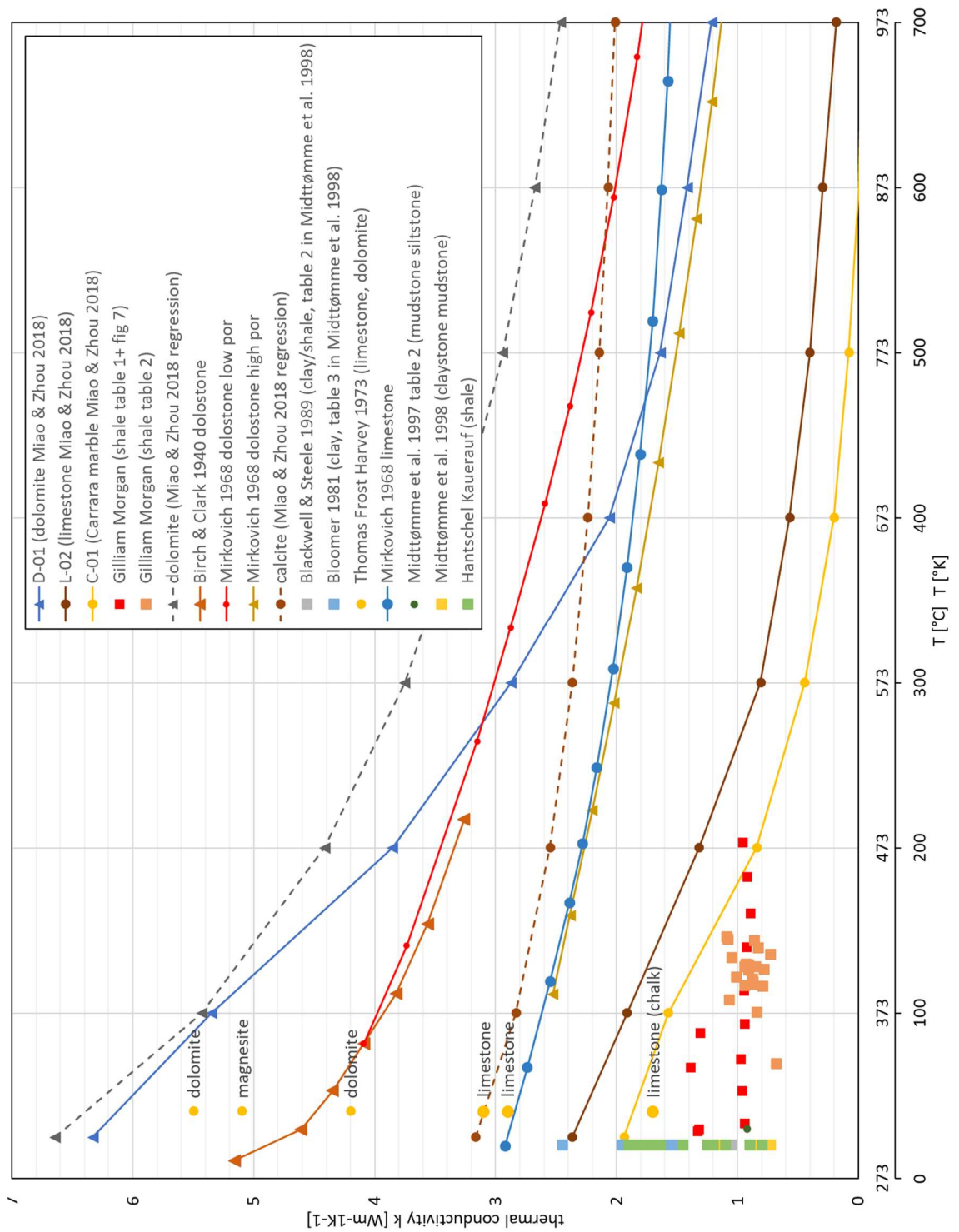
For the enhanced temperature model subject of this study all layers younger than Dinantian were replaced by those of the more recent DGM-Deep v5 model. This new version of DGM-Deep became available at the end of 2019. It is available via www.nlog.nl/en/geological-maps. The DGM-Deep v5 model is an update of DGM-Deep v4. Improved seismic interpretations and an updated velocity model were used for v5. The layers that are differentiated within DGM-Deep v5 are largely the same as those present in DGM-Deep v4, the only difference being that in v5 the Upper (RN) and Lower (RB) Germanic Triassic are present as separate units, while in v4 they were represented as a single unit. Because v5 became only available in a late stage (end of 2019) the Upper and Lower Germanic Triassic are still present as a single unit in the new temperature model. On a national scale, in the 3D grid of the temperature model, the differences between the two versions can be considered relatively minor. Therefore, the update from v4 to v5 is considered to have a relatively minor influence on the temperature model from surface level down to the base of the Rotliegend Group.

A new top of the Namurian as available in the DGM Deep v5 model was also included in the 3D grid of the enhanced temperature model (see Figure 4.13 and Figure 4.14). Differences with the previous version are mainly the result of an update of the time-depth conversion model. Because of considerations as described in paragraph 4.2.2, this enhancement can have a large influence on the modelled temperature in the Dinantian. Figure 4.14 shows that the depth of the top of the Namurian can locally be up to more than 1000 metres deeper (north-western part) or shallower (south-eastern part). This means that, depending also on the depth of the top of the Dinantian, the thickness of the Namurian will also change, which will influence the temperature at the top of the Dinantian, because of the insulating character of the Namurian rocks. That is, generally speaking, a thicker Namurian (in combination with an unchanged Westphalian) leads to a warmer Dinantian.

For the Dinantian the new maps as obtained in the SCAN study reported in [ten Veen et al. (2019)] were applied in the 3D grid of the temperature model. Figure 4.15 and Figure 4.16 show that considerable depth differences exist for the Dinantian between the prior (2018) and enhanced temperature model. This will lead to large differences in the calculated temperatures. Like the Namurian, the depth in the South-East is up to 1000 metres shallower, leading to a Dinantian which is up to about 30 °C cooler. On the other hand, in the largest part of the country the depth of the Dinantian is considerably larger (often between 1000-2000 metres but also up to 5000 metres over large areas. Obviously, the depth has remained the same in areas where well control existed.
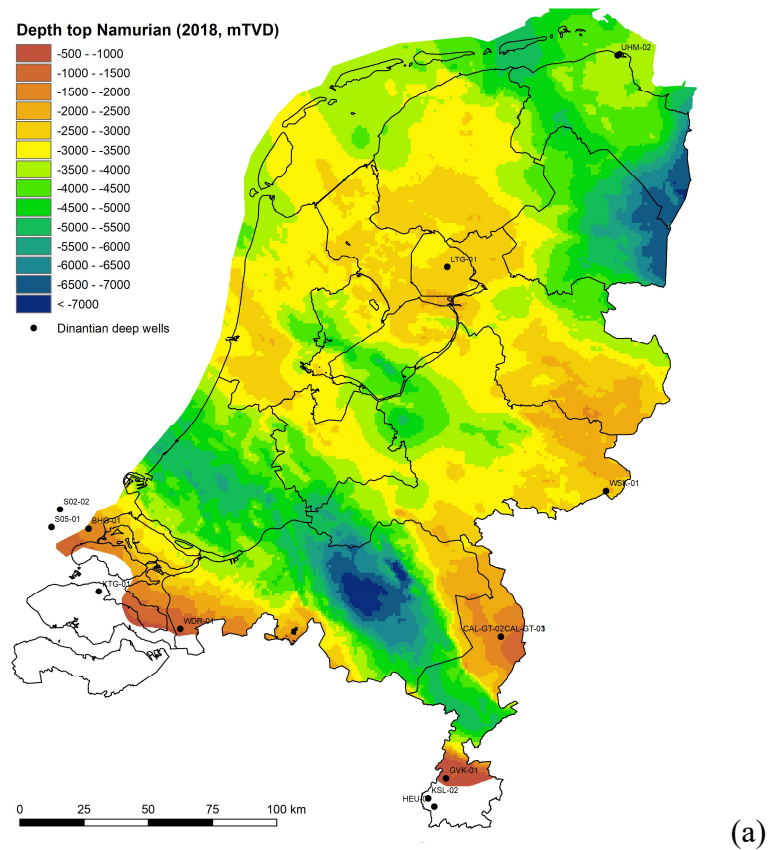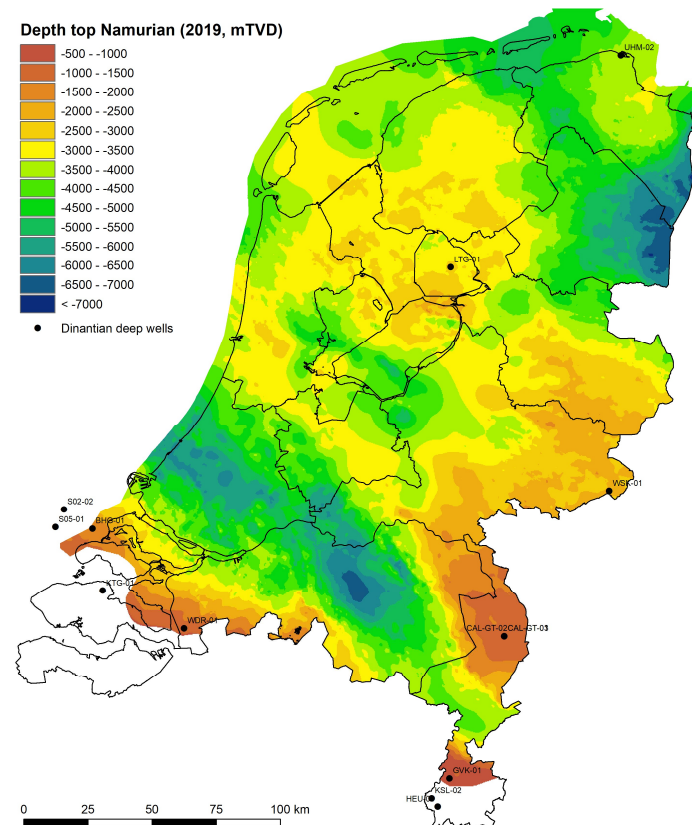
Figure 4.13   Depth to top Namurian (mTVD), prior (a) and enhanced temperature model (b)
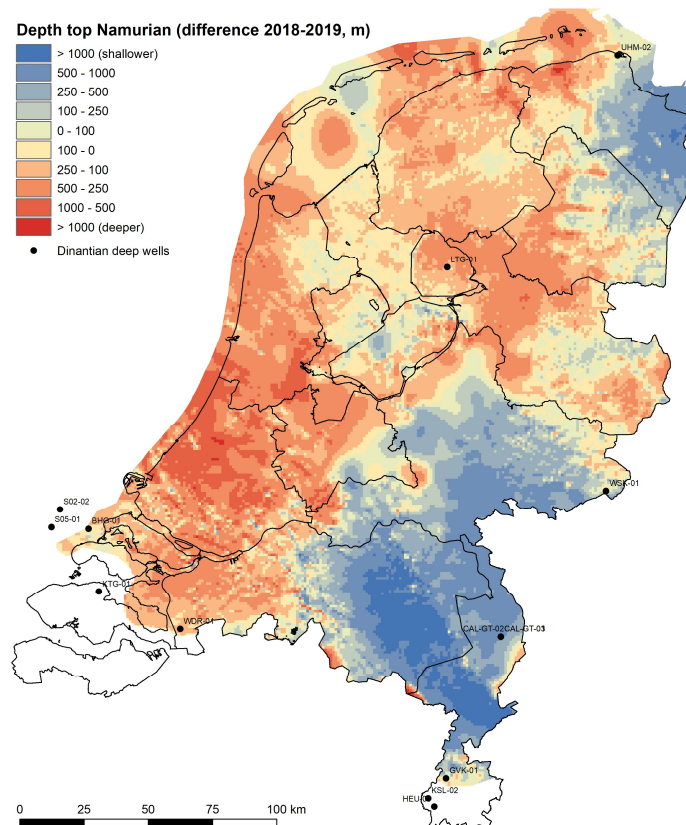
Figure 4.14   For prior (2018) and enhanced (2019) temperature model: Difference in
depth to top Namurian, 2018-2019 (blue: shallower, red: deeper)

The fact that the Dinantian was not drilled in the largest part of the country, and the
large uncertainties in the velocity model, imply that the depth of the Dinantian is
very uncertain, and hence the temperatures to be obtained.

The distinction, as made for the prior (2018) temperature model, between 'platform'
and 'basin' and as shown in top map of Figure 4.18 and obtained from [Boxem et al.
(2016)] was roughly based on elevation and (a change in) slope for the Groningen,
Friesland and Luttelgeest platforms. For the central part of the Netherlands, platform
presence was based only on the presence / absence of rocks belonging to the Chalk
Group. For the southern part of the Netherlands the maps published in [Reijmer et al.
(2017)] were used, resulting in Figure 4.18 (a). The thickness was assumed to be
constant (700 metre). The new facies map from [ten Veen et al. (2019)] includes
more legend entries (Figure 4.18, b) in the basinal facies. The base of the basin facies
is very poorly mappable as a seismic reflector. Therefore, the thickness should be
considered as indicative only, even as the basin facies may also be absent at some
places. For the enhanced temperature model subject of this study, the facies map of
ten Veen et al. (2019)] was simplified in platform / slope versus basinal (units 12 and
13 in Table 3.1).

Figure 4.19 shows a vertical North-South cross section through the 3D model. The
main units are colour coded according to Table 3.1.
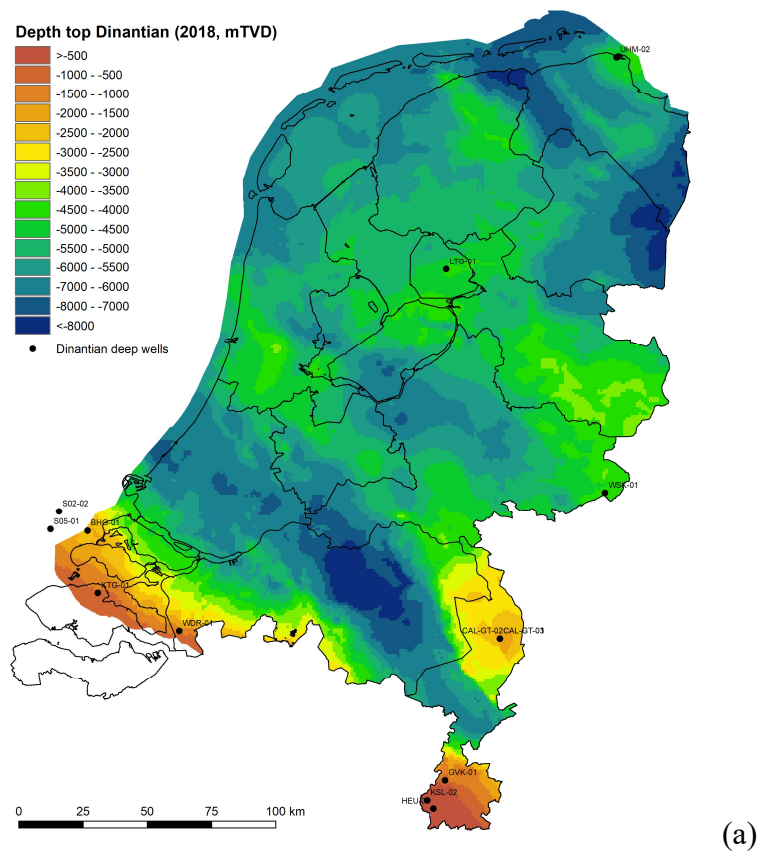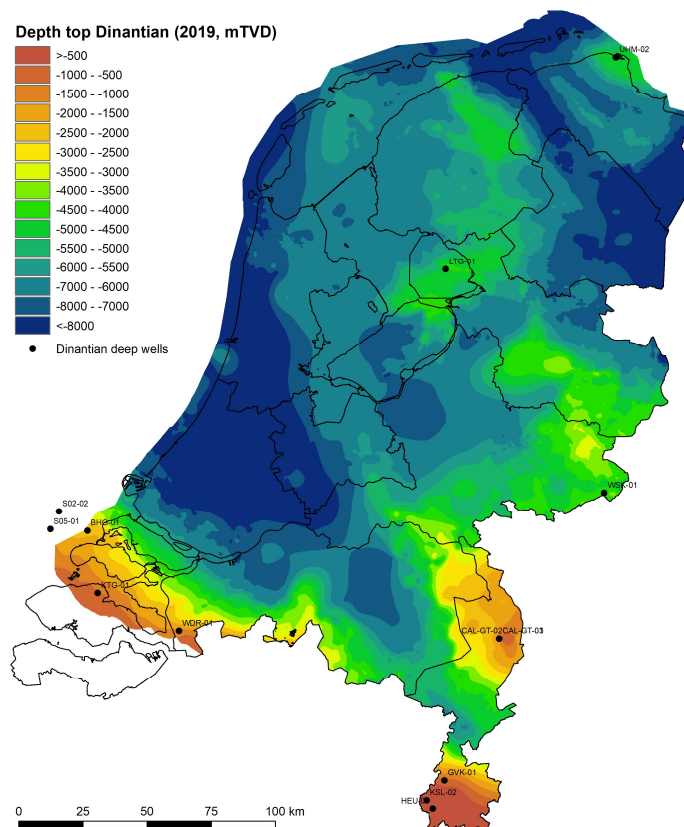
Figure 4.15   Depth to top Dinantian (mTVD) for prior (2018, a) and enhanced (2019, b) temperature model
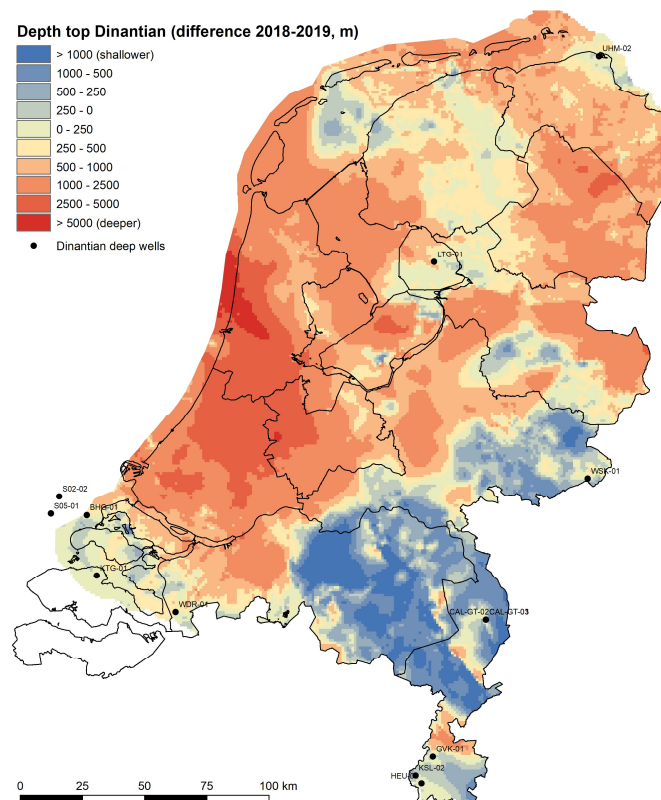
Figure 4.16   Difference in depth to top Dinantian (blue: shallower, red: deeper) for prior (2018) and enhanced (2019) temperature model.
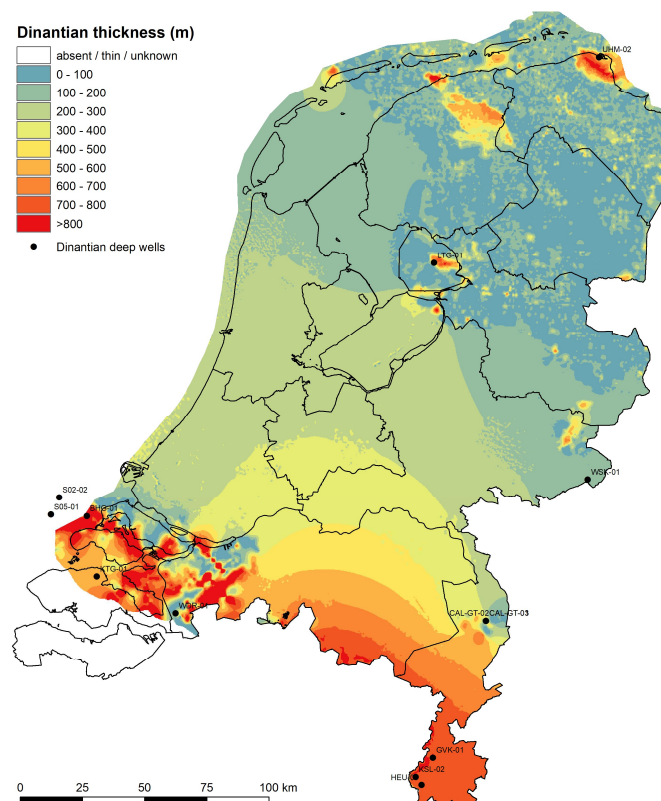
Figure 4.17   Thickness Dinantian as applied in the enhanced temperature model. The thickness between ~0 and ~400 metre in the basinal areas (Figure 4.18) is very uncertain.

54

Dinantian facies (2018)

- ▨ shelf interior / margin / slope
- ▨ basin
- ● Dinantian deep wells

0   25   50   75   100 km

(a)

Dinantian facies (Livian-Molinacian)

- ▨ platform carbonates (inc outline)
- ▨ platform carbonates (uncertain)
- ▨ basinal (condensed)
- ▨ basinal structural high
- ▨ basinal structural high (uncertain)
- ● Dinantian deep wells

0   25   50   75   100 km

(b)
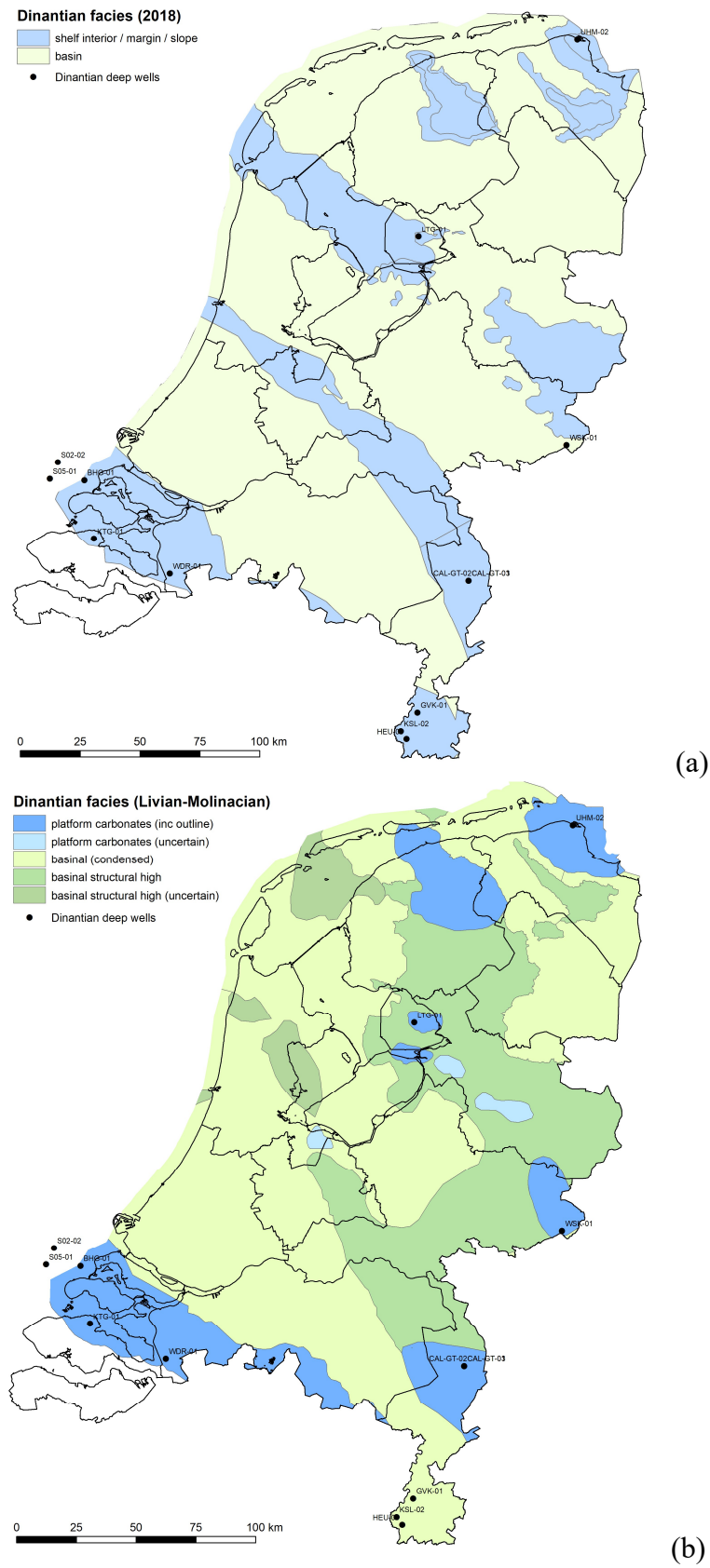
Figure 4.18   Facies Dinantian, prior (a, from [Boxem et al. (2016)] and enhanced (b, simplified from [Mozafari et al. (2019)] temperature model.

55
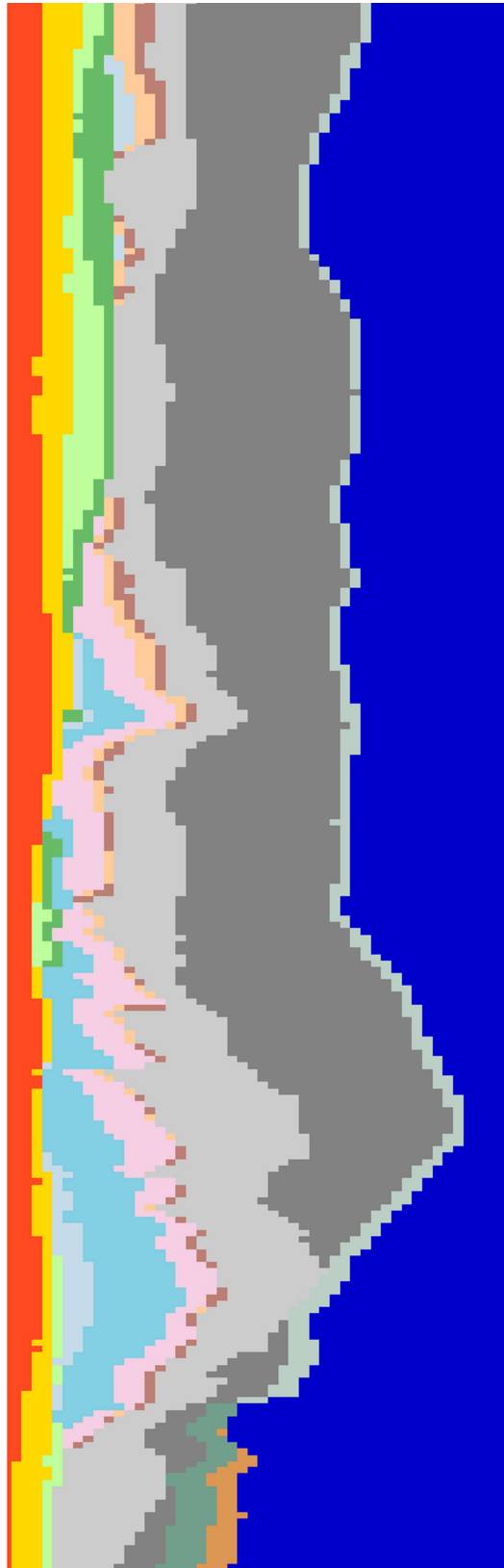
Figure 4.19   Southwest – Northeast cross section through coarse resolution model
(workflow steps 1-4), showing the geological units with colour coding as
Figure 3.1, Depth of the cross section 10 kilometres, length 240
kilometres, resolution 1000 metre horizontal, 200 metre vertical.

5 Resulting Dinantian temperature distribution

The enhanced temperature model for which the workflow has been explained in chapter 2, the main prior and additional temperature measurements, other new data, and prior and new modelling aspects that were discussed in chapters 3 and 4, provided a new resulting temperature distribution for the Dutch subsurface.

This new temperature distribution is subject of this chapter. First, the inversion is considered for a subset of the additional measurement data that became part of the temperature model. In a second section the temperatures as obtained for the Dinantian are being discussed.

5.1 Inversion applied to well ZRP-03

Figure 4.8 shows that for the Zeerijp location a large difference exists between the prior (2018) temperature model and the DTS temperature measurements. This could be caused by various factors, or more likely by a combination of two or more:

- Glaciations that occurred within the last 150,000 years. [Gies (2019)] argues that the shallow part of the subsurface still shows the effects of this cooling. The effect is most prominent in the first few hundreds of metres, but remains visible down to a depth of about 2000 metres.
- Erroneous values of the authigenic heat production (A), the vertical thermal conductivity (KV) and possibly the heat flow (HF);
- The use of potentially biased data for the 2018 temperature model.

Figure 5.1 illustrates the importance of having good temperature measurements, and the strength of the temperature model inversion procedure. This figure shows the results obtained for a 3D high-resolution grid centred around the Zeerijp-3 well for both the prior (2018) and the enhanced temperature models. For the prior (2018) temperature model no measurement data was available from the Zeerijp-3 well. The temperature gradient of the first ~300 metres is low. Further down, the temperature gradient in this area is anomalously high, like shown by the green curve, with respect to the average curve (black hatched line). The inversion for the prior (2018) temperature model produced a temperature gradient exceeding the Dutch average, illustrated by the red curve. Obviously the detailed Zeerijp-3 profile could not be reproduced properly, resulting in a large temperature difference between measurements and model over a large part of the vertical section.

Using the ZRP-03 temperature measurement data, the inversion for the enhanced temperature model was able to optimize the relevant rock properties (authigenic heat production and thermal conductivity) and heat flow in such a way that the observed temperature profile could be reproduced correctly, like illustrated by the blue curve.

In order to obtain a better fit of the temperature profile, the thermal conductivity values of the Upper and Middle/Lower North Sea Groups were adjusted in the inversion. The prior assumption for both units was a net-to-gross of 50%. Sand has a higher thermal conductivity than shale (see Table 3.3,

Table 3.4). Therefore, a high net-to-gross will results in a high value of the bulk thermal conductivity, and a low thermal gradient.

The thermal conductivity of the rocks belonging to the Upper North Sea Group was increased by a factor of 1.4. This could be representative of a higher net-to-gross. A vertical cross section through the REGIS[5] model at the Zeerijp location suggests that the shallow subsurface down to a depth of ~200 metres contains more sand than shale, but down to about 300 metres a thick clay is suggested (the depth of the base of the Upper North Sea Group is slightly over 300 metres). The effect of having a higher net-to-gross, resulting in a lower temperature gradient, has an effect similar to the glacial cooling. From this inversion exercise it cannot be concluded which of the two is more important. For geological reasons, it is likely that both are important.

The thermal conductivity of the Middle/Lower North Sea Group was lowered by a factor of 0.8 (indicative of a lower net-to-gross). Indeed, a net-to-gross map based on the cumulative Paleogene reservoir thicknesses available in the geothermal information system ThermoGIS[6] indicates that the net-to-gross in the area is closer to 25% than to the initially assumed 50%.

The decreased thermal conductivity of this layer also implies that the thermal gradient in the Lower and Middle North Sea Group interval is increased, which helps in matching the modelled top Rotliegend temperature and other additional temperature data. It also has influence on the Upper Carboniferous temperature gradient required to reach the high temperature in the Dinantian.

On a national level, the inversion exercise also has implications. Initial assumptions regarding the lithological composition of the North Sea Group were wrong. This has effect on the shallow temperature gradient, which directly influences the deeper temperatures. Generally speaking, an under-estimation of the shale content of the sediments will also under-estimate the geothermal gradient and therefore the temperatures at larger depths. The issue of net-to-gross value was addressed for the current study by changing the prior net-to-gross values for the North Sea Group. From the constructed net-to-gross maps of the Upper and Lower / Middle North Sea Groups it becomes clear that the lateral variation is large. While the ES-MDA algorithm is able to locally vary prior property values, better results are obtained when the prior estimates are closer to the true values. Obviously, lateral variation of

---

[5] REGIS is the REgional Geo-hydrological Information System, available from www.dinoloket.nl/en/subsurface-models. The maximum depth of this 2.5D model in the Zeerijp area varies between ~270 and ~480 mNAP.
[6] www.thermogis.nl/

the lithological composition is not limited to the sediments in the North Sea Group. Currently, it is not possible in the modelling to use maps representing the lithological variation within a unit. It is clear that enabling this may significantly improve the temperature estimates.
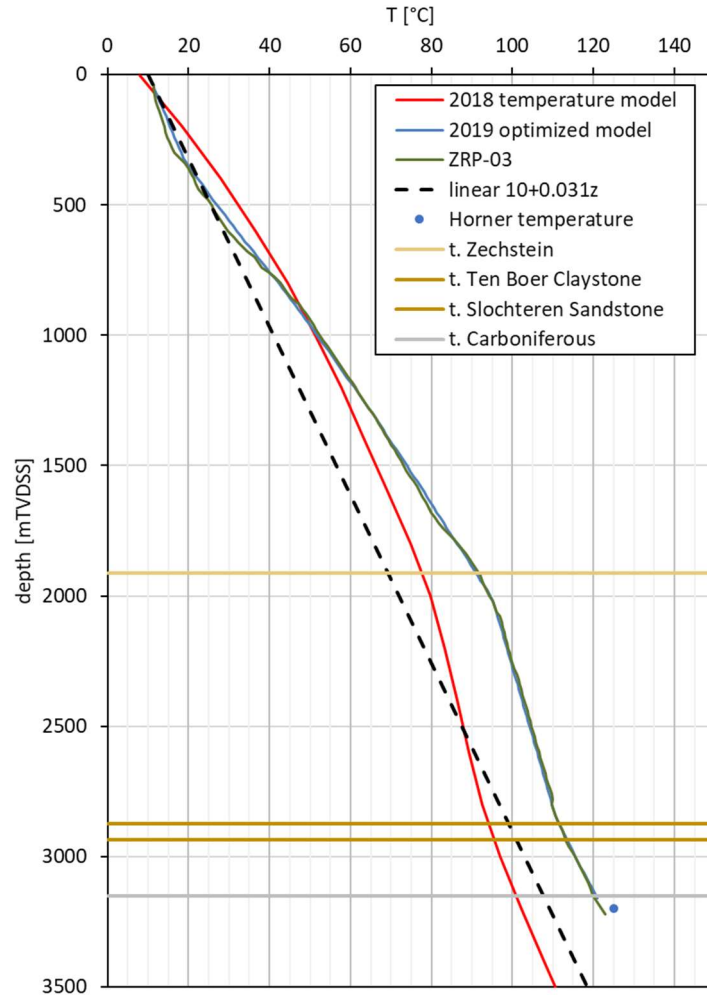
Figure 5.1   Results of inversion for the enhanced temperature model for well ZRP-03 using DTS-data for this well.

5.2 Temperature at top Dinantian depth

Figure 5.2 shows the main result of this study, the temperature distribution at the top of the Dinantian reservoir, obtained with the enhanced temperature model, together with the temperature obtained with the prior (2018) model.

The temperature at other key depths or horizons can also be extracted from the enhanced temperature model. Due to the improvements in the model as a whole, described in previous chapters, the temperatures (and therefore also the temperature gradients) at depths shallower than the Dinantian are also an improvement over the previous versions of the temperature model. The most important factors which were

changed in shallower layers and which contribute to the improved temperature estimate of the Dinantian are:

- the improved lithological composition estimate of the North Sea Group sediments;
- the additional temperature measurements in the Groningen area;
- the improved depth map of the top of the Namurian;
- the improved estimates of the thermal conductivity values of the Upper Carboniferous strata.

Only the results for the Dinantian, which was the target of the current study, are considered here. The most striking differences are caused, to a large extent, by the updated depth of the top Dinantian surface, which is considerably deeper in large parts of the country for the updated version. Notably, areas where the temperature in both versions of the model remained the same are the areas where the depth of the Dinantian has remained the same and because temperature measurement data was already available, at least for the depth of the Dinantian. Note that a larger high-quality display of the bottom map of Figure 5.2 is found in Appendix B

It is not straightforward to assign an uncertainty level to temperature distribution obtained for the Dinantian. The ES-DMA aims at minimizing the difference between observations (measured temperature) and model. Therefore, the difference between the two is not a measure of the quality of the model, but of the ability of the ensemble smoother. The temperature model is based on physics, but the uncertainty about many of the input data sources is considerable. Judging from the Zeerijp DTS data, a difference between modelled and measured temperature may be up to 20 °C. Various factors contribute to the uncertainty of the temperature estimate:

- Temperature observations. Very few temperature measurement data are available at the depth of the Dinantian. Most of which have low accuracy. Therefore, the temperature of the Dinantian is poorly known. A temperature model with a minimum estimation error at the location of the temperature observations (which is the goal of the data assimilation) still has uncertainty at those locations. Further away from the temperature observations, the uncertainty is even larger.
- Depth of the Dinantian. The model does not take uncertainty of the depth of the Dinantian into account. This is a major drawback because there is large uncertainty in the depth. A difference of 1000 metres, which is not uncommon when considering Figure 4.16, would already account for ~30 °C temperature difference. Layers in DGM-Deep v5 are published with an associated uncertainty map resulting from uncertainties in structural complexity, quality of the seismic pick, and the velocity model. This product is not yet available for the Dinantian.
- Rock properties such as thermal conductivity and authigenic heat production, and heat flow - Those properties are also poorly known. The data assimilation attempts to minimize the difference between temperature observations and modelled temperature by changing the rock properties and heat flow within reasonable limits. Different combinations of rock properties and heat flow may

produce similar results, but it is not known which properties are the correct ones. Especially poor-quality temperature observations may trigger incorrect rock property values and thereby incorrect temperature predictions.
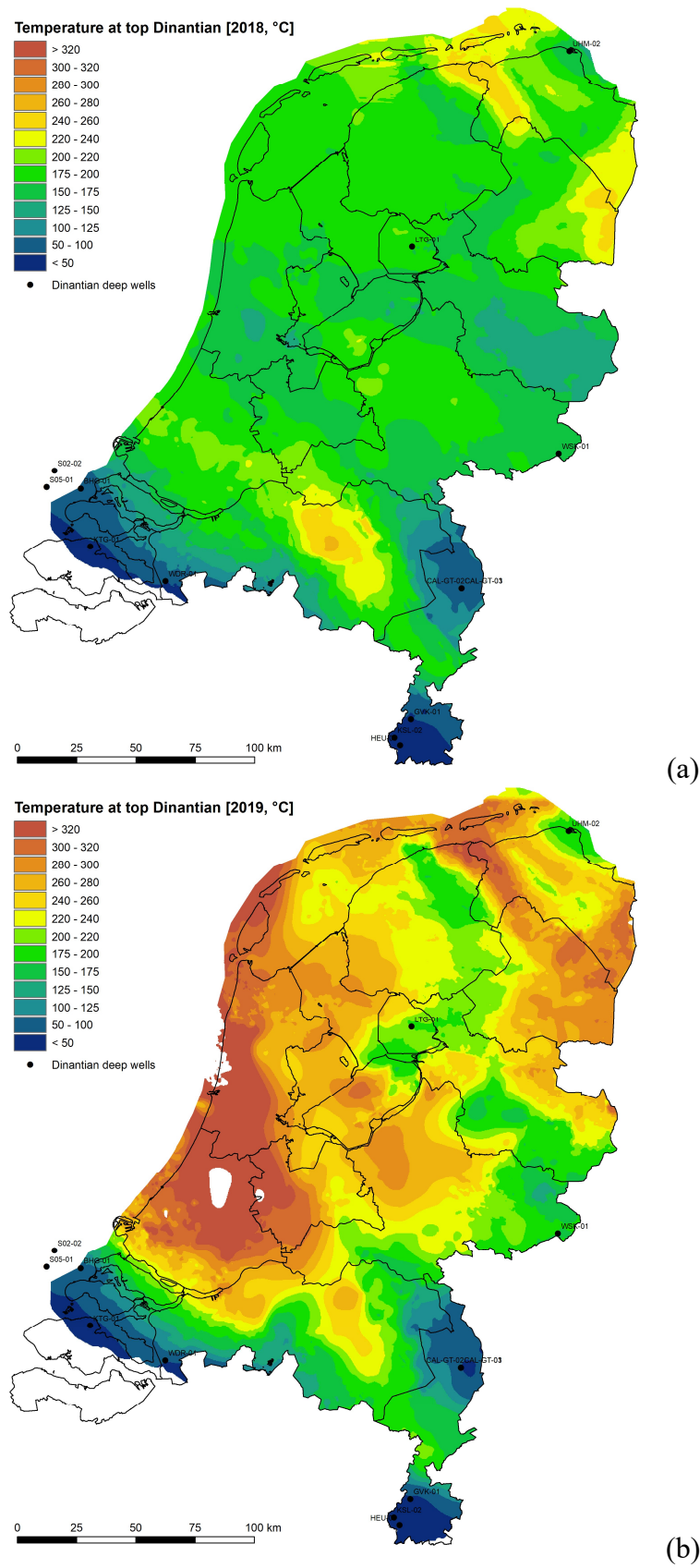
Figure 5.2   Temperature at top Dinantian level for prior (2018, a) and enhanced (2019, b) temperature models. White spot: depth > 10 kilometres.

62

6 Discussion, conclusions and recommendations

An enhanced temperature model has been developed in this SCAN study, specifically for generating a better estimate for the temperature distribution in the Dinantian carbonates in the Dutch subsurface. In order to arrive at a better temperature estimate for the Dinantian, improvements were also made to data relevant for younger strata. In this last chapter only conclusions are drawn on what this study has obtained for the Dinantian. The chapter concludes with several recommendations for further work, which are not specifically for temperature modelling for the Dinantian but for such modelling in a more general sense.

6.1 Conclusions

In this SCAN study an enhanced temperature model was developed, which is a major improvement over the prior (2018) model at the depth of the Dinantian because of the following reasons:

- Improved maps of all geological units were accounted for such as the DGM Deep v5 geological model for the units down to Rotliegend level, an updated depth of the top of the Namurian map, and (most importantly) maps of the top and bottom depth of the Dinantian reservoir as obtained in another SCAN study;
- The facies distribution for the Dinantian, also resulting from another SCAN study, was applied as important information for the model, helping to better determine the relevant rock properties;
- Derived Horner corrected temperature data at Dinantian level, obtained in one of the other SCAN studies, were added to the database with temperature measurements and used in the temperature modelling;
- For the Groningen area, a large dataset of reliable temperature measurements at Rotliegend level was added to the model database with temperature measurements and used in the temperature modelling;
- A literature review in combination with a 1D temperature modelling exercise was executed to determine which thermal conductivities best fit the Westphalian, Namurian and Dinantian rocks.

The temperatures modelled for the depth of the Dinantian are higher in the largest part of the Netherlands compared to temperatures obtained with the prior (2018) model. This is partially caused by the depth of the Dinantian reservoir, which is deeper in a large part of the Netherlands than was the case for the prior model. Also, the selected value of the thermal conductivity of the rocks directly overlying the Dinantian has influence on the temperature of the Dinantian rocks because of its insulating nature. In this study it has been concluded that convection does not play a role in the temperature development of the Dinantian rocks.

The uncertainty of the modelled temperature at the top of the Dinantian is large. There are few measured temperature data points at this level. The available data

points are Horner corrected bottom hole temperatures, which typically have an accuracy of ±10°C. Additional temperature measurements and rock thermal property measurements are considered to be the best way to decrease the uncertainty of the temperature estimate. When no reference temperature data are available the accuracy of the model cannot be assessed easily but for the Zeerijp case where good data has become available the error at largest depth is about 20 °C.

The factors that have the largest influence on the temperatures at Dinantian level are depth, thermal conductivity, heat flow and lithology (facies). It is well known that the velocity model is uncertain at large depths, due to the lack of sufficient time-depth data. Also, the interpretation of the top Dinantian reflector is uncertain in large parts of the area due to the poor quality and density of the seismic data.

6.2 Recommendations for further work

New data first used in this study show a considerable mismatch with the prior (2018) temperature model and also a mismatch with the geothermal gradient calculated in [Bonté et al. (2012)]. As the focus of this study was the addition of deep layers to the temperature model, not all observed problems with the model in the shallower strata could be resolved. The Zeerijp case shows that at a depth of 2 km a temperature was measured that is over 20 °C higher than the Bonté trend, and about 14 °C higher than for the prior temperature model. This mismatch was resolved in the Zeerijp region in the enhanced temperature model, but similar mismatches may remain in the rest of the country, as no DTS data is available here.

The impact of such mismatches, if present, on planned geothermal projects would be large, as prediction of the production temperature forms an important part of the economic pre-drill evaluation of geothermal projects. In order to decrease the uncertainties in the temperature modelling at all geological levels, a number of activities is strongly recommended.

6.2.1 Depth of the Dinantian reservoir

The uncertainty of the depth of the Dinantian reservoir has a major influence on the temperature estimate. Different realizations of the top Dinantian surface (shallower and deeper), generated from variations of the velocity model, would result in lower and higher temperatures. Therefore, reducing this uncertainty will lead to a more reliable temperature estimate. This requires that more well data are acquired (from new wells) to allow for a better control of depth and time (sonic logs and wellbore seismic).

6.2.2 Temperature measurement data

The quality of the model database with temperature measurements, which consists mostly of BHT data, at shallower depth than the Dinantian, is an issue. Various authors draw attention to the inaccuracy of corrected bottom hole temperatures, and that they tend to be biased towards lower temperatures. Attention should therefore be

paid to establishing a more reliable temperature measurements database, which includes further collection of measurements, a more transparent BHT correction method, and includes the assessment of the potential bias in measurement data.

Additional temperature measurement data should not only become available from new wells though, of which only a few are being drilled annually to large depth. The fact that in the coming decades hundreds of existing hydrocarbon production wells will be abandoned offers a huge opportunity for obtaining additional and reliable temperature data. Existing wells are in temperature equilibrium with the reservoir, and the recording of a DTS profile using fibre optic technology is relatively quick and cheap. The resulting temperature profile does not require correction. Additional temperature measurement data (like the Zeerijp DTS data applied in this study) is not only very valuable for improving the temperature estimate of the model, but also important for better estimating the relevant rock properties and heat flow.

It is known that not all temperature data in the model database with temperature measurements is currently fully unlocked. This data concerns:

- Temperature logs (non-equilibrium), considered to be valuable because these are recorded over longer well sections. Their correction to equilibrium, however, is complicated and potentially biased. Extracting this data from the database of NLOG with log reports (digitizing and correcting) is time consuming.
- BHT, mainly from wells that have not been examined for temperature data so far. The added value is considered to be limited though, because wells in white areas have been examined already and wells that have not been examined so far are in data dense areas.

Various operators that operate onshore, like NAM, from which several datasets were used in this study, most likely also have more data of (equilibrium) well temperatures. These data are not compulsory submitted to TNO-AGE, as is required for other types of data in the Mining Law, and are therefore not present in the subsurface database maintained by TNO. However, such data could be a valuable addition to the model database with temperature measurements.

6.2.3 Rock thermal properties

Thermal properties of all rocks involved are crucial for the quality and accuracy of temperatures obtained with the model subject of this study. Such properties can be measured directly from core material or estimated from well logs. Also, lithology can be used as an estimator for those properties. These methods have not been employed to the full extent so far. A study of well logs can also provide more information on the lithological variation within a model unit.

6.2.3.1 Measurements from cores or well logs

The thermal properties that are used in the current temperature model general originate from [Hantschel & Kauerauf (2009)]. Literature may further help to obtain

65

better (local) conductivity values, including values that are measured on actual rocks. Furthermore, several hundreds of kilometres of cores are available from the TNO core shed. This material could be used for better estimating thermal properties, provided it was properly conserved; dried out core and cutting material is probably not representative of the subsurface. Additionally, it is possible to estimate thermal conductivities from geophysical well logs. [Fuchs & Förster, (2013); Fuchs et al. (2015)] propose methods to calculate thermal properties from gamma ray, density, sonic interval transit time, hydrogen index and photoelectric factor in combination with relevant rock properties such as shale fraction, matrix hydrogen index and matrix density. These methods may be less accurate than direct measurements on core material, but their application may lead to the addition of thermal property estimates for many kilometres of logs. [Dalby (2018)] applied the methods proposed by [Fuchs & Förster, (2013); Fuchs et al. (2015)] to Dutch wells, and also measured thermal properties on core material from those wells. The method appears promising but has not been implemented yet. The potential of these logs is therefore not used yet and should be unlocked by systematically measuring properties on core material and estimating them from logs.

Well based inversion may lead to an improved calibration of the temperature model in case reliable temperature logs become available (like for the well Zeerijp-3 for this study), Well based inversion also leads to an improved understanding of the rock properties at the well locations, which in turn can be used to generate rock property maps that capture trends. Therefore, it is recommended that temperature logs should also become available to improve the rock property estimates.

6.2.3.2 Lithology as a proxy for rock properties

The lithological composition of the units in the temperature model varies laterally. This results in a bulk thermal conductivity that also varies laterally. Until now, the lithological composition is given per model layer on a national scale. Improved knowledge on lateral variations will lead to better prior and posterior models. Little information is available concerning the lateral and vertical lithological variation.

Lithological information can be derived from cutting descriptions, lithologs and/or well logs, all of which are available in the database of NLOG. This information is not yet unlocked but is ready for processing on a national level (and which means extraction of this information from the database in a consistent way including quality checking). Machine learning techniques could prove valuable for extracting relevant information from this heterogeneous dataset.

Net/gross estimates can be derived from well logs, especially gamma ray, but not yet in a (semi-)automated fashion. The development of machine learning techniques may be of help here. Using net/gross estimates derived from log data large scale variations in lithological composition can be visualized. This would improve the estimation of prior thermal properties, which is especially important for those units or Formations that are heterogeneous in character, and contain lithologies with

strongly differing thermal properties. Candidates are the North Sea Group (mostly sand, silt and shale), the Triassic (sandstone and shale) and the Upper Carboniferous (shale, with lesser amounts of silt and sand, and coal). For these units, the net-to-gross could be determined using gamma ray logs. Currently, this cannot be done in an automated fashion with high accuracy. The application of machine learning techniques may help. Within the Zechstein, rock salt has a high thermal conductivity which causes a low thermal gradient. There is a large areal variation in composition of the Zechstein, including rock salt, clay, anhydrite and carbonates. General maps exist of their lateral occurrence, but not vertical. This information could also be derived from well logs.

6.2.4 Accuracy of the model

No comprehensive assessment of the quality of the model has been carried out yet. Further to the recommendations in section 6.2.2 on the measurement data used, it is recommended to assess the temperature model by performing a comparison of results with additional measurement data or measurement data omitted in the model runs. Differences observed between temperature estimates from the model and measurement could hint on improvements for the thermal calculations & required input, the inversion procedure or for (better) measurement data in specific areas.

Furthermore, it is also believed that further use of the results of the enhanced temperature model will produce feedback from users on its accuracy. Therefore, it is recommended that such results are part of the next update of in the geothermal information system ThermoGIS.

7 References

Balling, N., Poulsen, S. E., Fuchs, S., & Mathiesen, A. (2016). Development of a numerical 3D geothermal model for Denmark. European Geothermal Congress

Batzle, M., & Wang, Z. (1992). Seismic properties of pore fluids. Geophysics 57: 1396-1408.

Békési, E., Struijk, M., Bonté, D., Veldkamp, J. G., Limberger, J., Fokker, P. A., Vrijlandt, M., & Van Wees, J. D., in prep. An updated geothermal model of the Dutch subsurface based on inversion of temperature data.

Blackwell, D. D., & Richards, M. (2004). Calibration of the AAPG Geothermal Survey of North America BHT Data Base. AAPG Annual Meeting

Bonté, D., Van Wees, J. D., & Verweij, H. (2012). Subsurface temperature of the onshore Netherlands: new temperature dataset and modelling. Netherlands Journal of Geosciences 91 (4): 491-515.

Boxem, T. A. P., Veldkamp, J. G., & Van Wees, J. D. (2016). Ultra-diepe geothermie: Overzicht, inzicht en to-do ondergrond. Published by TNO and available via www.tno.nl/media/9728/tno_udg-ondergrond_r10803.pdf.

Cannon, M., & Kole, P. (2018). The First Year of Distributed Strain Sensing (DSS). Monitoring in the Groningen Gas Field. Report No. SR.17.00934, Published by NAM and available via nam-feitenencijfers.data-app.nl/download/rapport/0c9646b5-28e5-401a-949f-a680c29b896a?open=true.

Burkitov, U., Van Oeveren, H., Valvatne, P., van Elk, J., & Doornhof, D., (2016). Groningen Field Review 2015 Subsurface Dynamic Modelling Report. Report No. EP201603238100, published by NAM and available via nam-feitenencijfers.data-app.nl/download/rapport/e683753a-e085-417d-995d-b7ae7a9c820f?open=true

Carlson, T. (2019). Petrophysical Report of the Dinantian Carbonates in the Dutch Subsurfaceacies analysis and diagenetic evolution of the Dinantian carbonates in the Dutch subsurface. Available via www.nlog.nl/scan.

Dalby, C. J. (2018). Characterisation of the thermal conductivity in the Netherlands. Master Thesis. Published by University of Utrecht.

De Jager, J., & Visser, C. (2017). Geology of the Groningen field - an overview. Netherlands Journal of Geosciences 96 (5): 3-15.
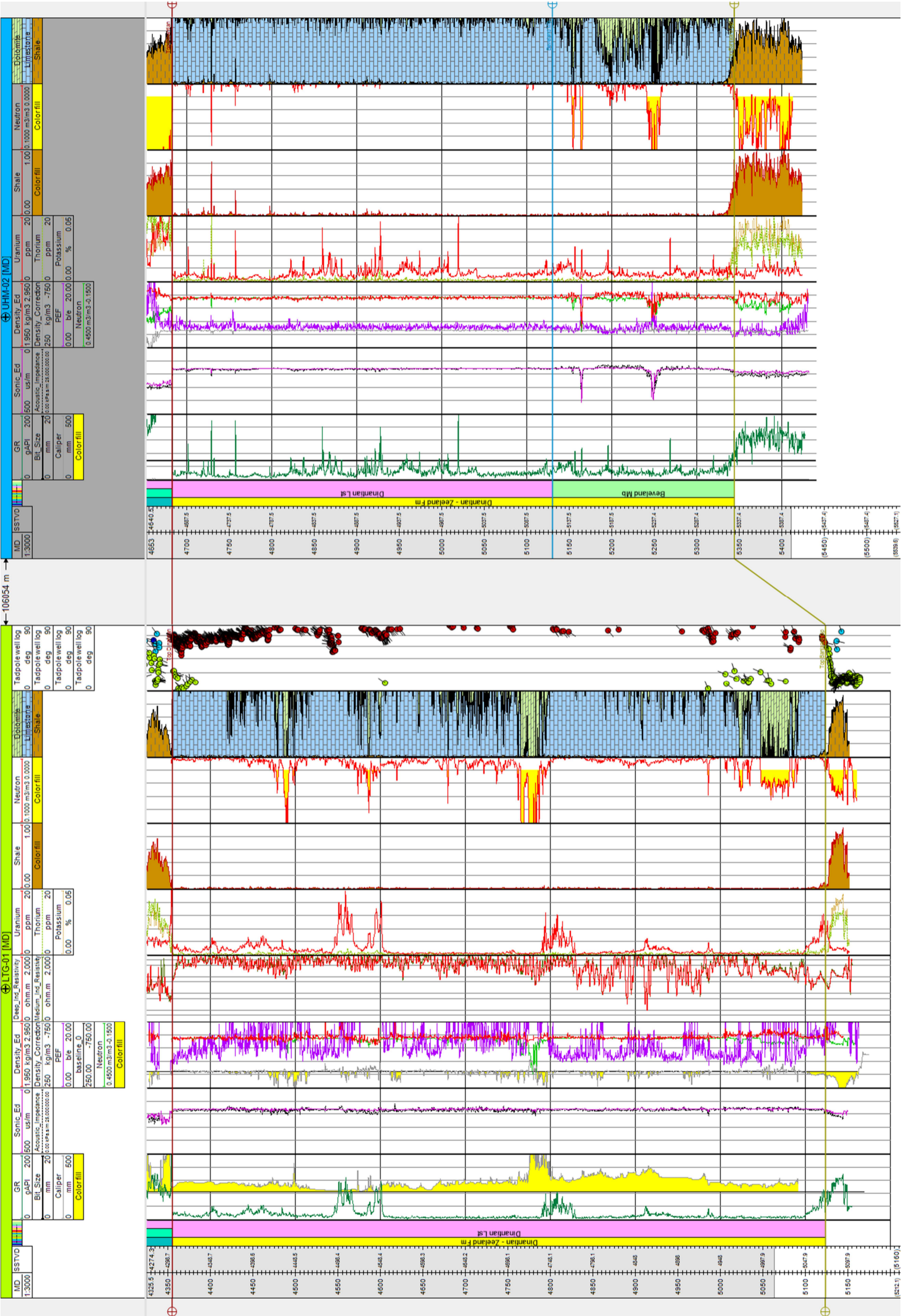
Emerick, A. A., & Reynolds, A. C. (2013). Ensemble smoother with multiple data assimilation. Computers & Geosciences 55: 3-15.

Fuchs, S., & Förster, A. (2014). Well-log based prediction of thermal conductivity of sedimentary successions: a case study from the North German Basin. Geophysical Jourmal International 196 (1): 291-311.

Fuchs, S., Balling, N., & Förster, A. (2015). Calculation of thermal conductivity, thermal diffusivity and specific heat capacity of sedimentary rocks using petrophysical well logs. Geophysical Journal International 203 (3): 1977-2000.

Fuchs, S. (2018). The variability of rock thermal properties in sedimentary basins and the impact on temperature modelling–A Danish example. Geothermics 76: 1-14.

Gies, C., 2019. The shallow subsurface thermal model of the Netherlands. Masters Thesis. Published by Utrecht University, Utrecht.

Goutorbe, B., Lucazeau, F., & Bonneville, A. (2007). Comparison of several BHT correction methods: a case study on an Australian data set. Geophysical Journal International 170 (2): 913-922.

Grunberg, L. (1970). Properties of sea water concentrations. Third International Symposium on Fresh Water from the Sea, Vol. 1

Hantschel, T., & Kauerauf, A. I. (2009). Fundamentals of basin and petroleum systems modeling Springer Science & Business Media.

Hermanrud, C., Cao, S., & Lerche, I. (1990). Estimates of virgin rock temperature derived from BHT measurements: Bias and error. Geophysics 55 (7): 924-931.

Hermanrud, C., Lerche, I., & Meisingset, K. K. (1991). Determination of virgin rock temperature from drillstem tests. Journal of Petroleum Technology 43 (9): 1126-1131.

Holzbecher, E. O. (1998). Modelling density driven flow in porous media: Principles, numerics, and software. Berlin, New York: Springer.

Kukkonen, L. T., Jokinen, J., & Seipold, U. (1999). Temperature and pressure dependencies of thermal transport properties of rocks: implications for uncertainties in thermal lithosphere models and new laboratory measurements of high-grade rocks in the Central Fennoscandian shield. Surveys in Geophysics 20: 33-59.

Lapwood, E.R. (1948). Convection of a fluid in a porous medium. Mathematical Proceedings of the Cambridge Philosophical Society, 508-521.

Lee, D. S., Park, K. G., Lee, C., & Choi, S. (2018). Distributed Temperature Sensing Monitoring of Well Completion Processes in a CO_2 Geological Storage Demonstration Site. Sensors 18 (4239)

Limberger, J., & Van Wees, J. D. (2014). 3D subsurface temperature model of Europe for geothermal exploration. 76th EAGE Conference and Exhibition

Lipsey, L., Pluymaekers, M. P. D., Goldberg, T., van Oversteeg, K., Ghazaryan, L., Cloetingh, S., & Van Wees, J. D. (2016). Numerical modelling of thermal convection in the Luttelgeest carbonate platform, the Netherlands. Geothermics 64: 135-151.

Mozafari, M., Gutteridge, P., Riva, A., Geel, C.R., Garland, J., & Dewit, J. (2019). Facies analysis and diagenetic evolution of the Dinantian carbonates in the Dutch subsurface: overview and synthesis. Available via www.nlog.nl/scan

Peters, K. E., & Nelson, P. H. (2009). Criteria to Determine Borehole Formation Temperatures for Calibration of Basin and Petroleum System Models. Search and Discovery

Reijmer, J. J. G., ten Veen, J. H., Jaarsma, B., & Boots, R. (2017). Seismic stratigraphy of Dinantian carbonates in the southern Netherlands and northern Belgium. Netherlands Journal of Geosciences 96 (4): 353-379.

Shen, P. Y., & Beck, A. E. (1986). Stabilization of bottom hole temperature with finite circulation time and fluid flow. Geophysical Journal of the Royal Astronomical Society 86: 63-90.

Shiina, Y. & Hishida, M. (2010). Critical Rayleigh number of natural convection in high porosity anisotropichorizontal porous layers. International Journal of Heat and Mass Transfer 53: 1507–1513.

Struijk, M. (2016). An improved method for modeling the subsurface of the onshore Netherlands. Master Thesis. Published by University of Utrecht.

Ten Veen, J. H., de Haan, de Bruin, G., P., Holleman & N., Schöler, W. (2019). Seismic Interpretation and Depth Conversion of the Dinantian carbonates in the Dutch subsurface. Available via www.nlog.nl/scan

Tesauro, M., Kaban, M., & Cloetingh, S. (2009). A new thermal and rheological model of the European lithosphere. Tectonophysics 476 (3): 478-495.

Ukil, A., Braendle, H., & Krippner, P. (2012). Distributed Temperature Sensing: Review of Technology and Applications. IEEE Sensors Journal 12 (5): 885-892.
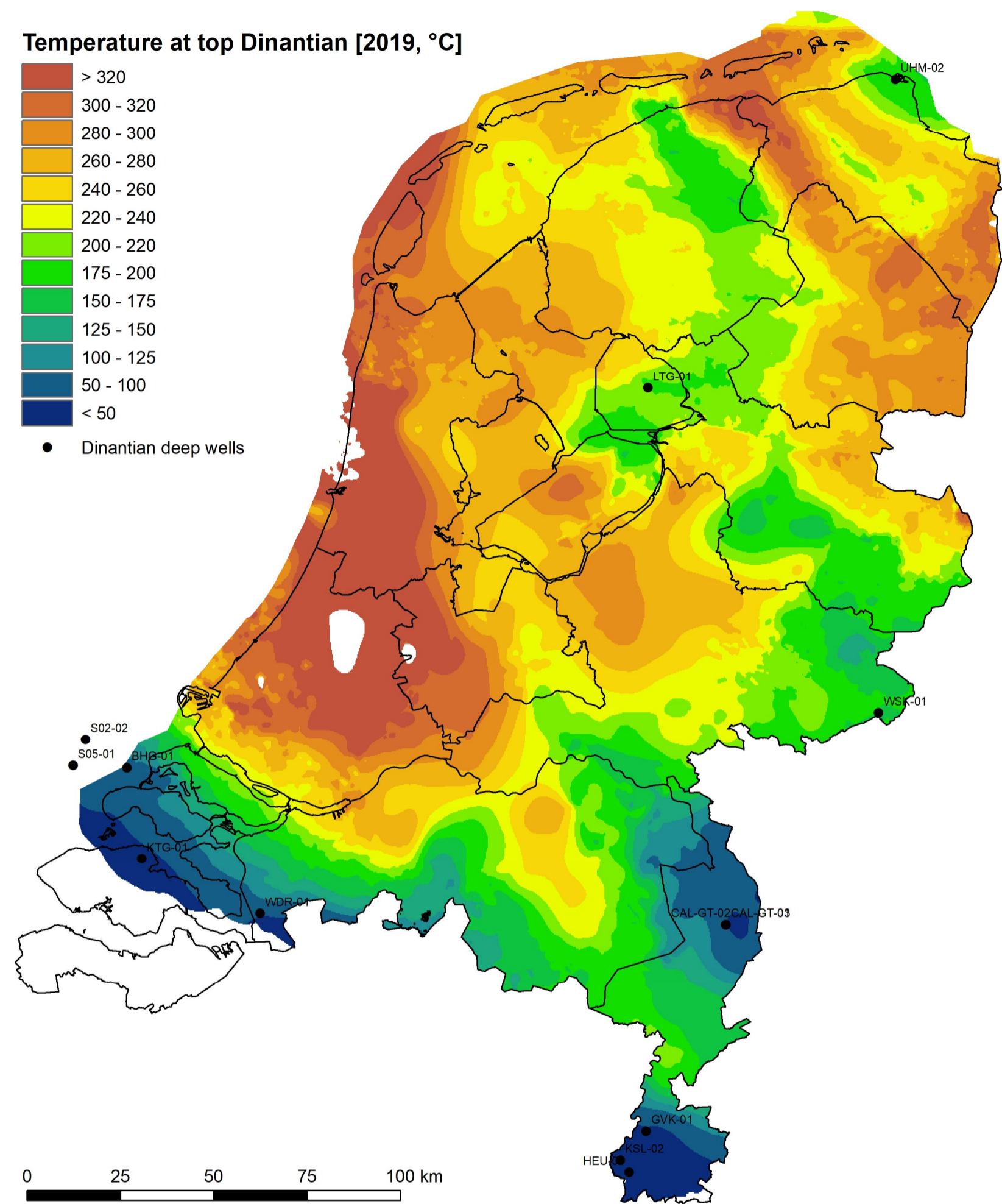
Van Leverink, D. J., & Geel, C. R. (2019). Fracture characterization of the Dinantian carbonates in the Dutch subsurface. Published on www.nlog.nl/scan

Van Oversteeg, K., Lipsey, L., Pluymaekers, M., Van Wees, J. D., Fokker, P. A., & Spiers, C. J. (2014). Fracture Permeability Assessment in Deeply Buried Carbonates and Implications for Enhanced Geothermal Systems: Inferences from a Detailed Well Study at Luttelgeest-01, The Netherlands. Proceedings Thirty-Eighth Workshop on Geothermal Reservoir Engineering, Stanford University, Stanford, California

Verweij, J. M., & Hegen, D., 2015. Integrated pressure information system for the onshore and offshore Netherlands. Report No. R10056. Published by TNO, Utrecht.

Waples, D. W., & Pedersen, M. R. (2004). Evaluation of Horner Plot-Corrected Log-Derived Temperatures in the Danish Central Graben, North Sea. Natural Resources Research 13 (4): 223-227.

Zhao, C., Hobbs, B. E., & Ord, A. (2008). Convective and advective heat transfer in geological systems of crustal scales. Berlin, Heidelberg: Springer-Verlag.

Appendix A: Well panel of LTG-01 and UHM-02

LTG-01 and UHM-02 wells showing the low porosity for the largest part of the Dinantian section, except for the dolomitized intervals. Data from [Carlson (2019); Mozafari et al. (2019)].

Appendix B: Temperature distribution at Top Dinantian

Temperature at top Dinantian [2019, °C]

- > 320
- 300 - 320
- 280 - 300
- 260 - 280
- 240 - 260
- 220 - 240
- 200 - 220
- 175 - 200
- 150 - 175
- 125 - 150
- 100 - 125
- 50 - 100
- < 50

● Dinantian deep wells

0   25   50   75   100 km

Appendix C: Influence of steel casing on near well bore reservoir temperature

During the project the question was raised how representative a downhole temperature measurement is of the reservoir temperature. A short study has therefore been performed on the influence of the steel casing on a temperature measurement obtained within a well. A model was set up which is considered to be characteristic for the Dutch subsurface. The geometry for this setting is shown in Figure C.1. It represents an axi-symmetric domain with the following three materials:

-   brine in wellbore (in blue)
-   subsurface rock (white)
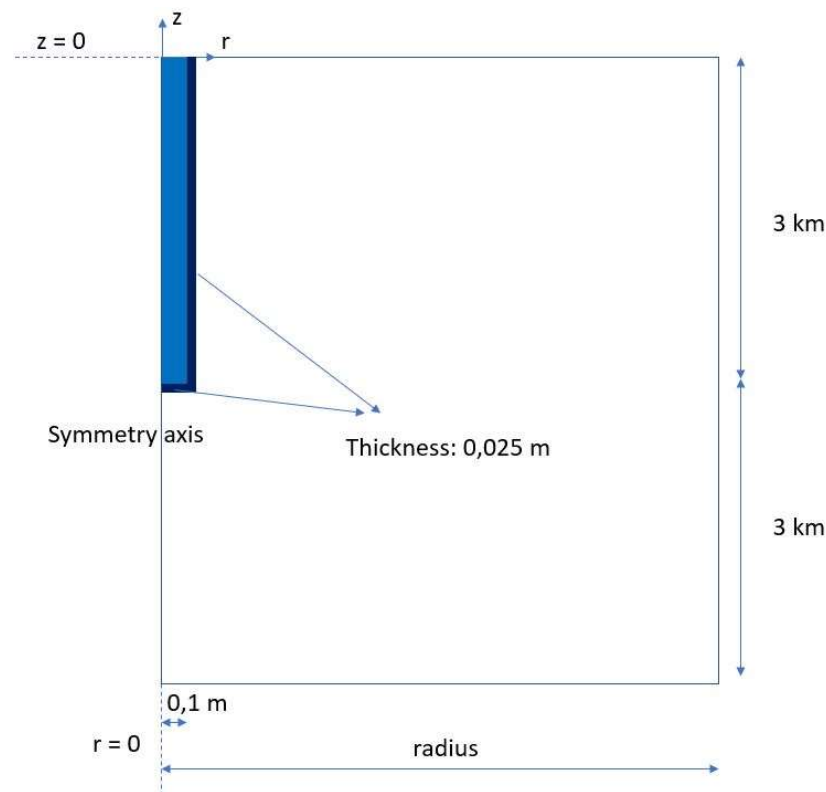-   casing material (in black).

Figure C.1   Geometry of characteristic subsurface setting with brine (blue), wellbore casing (black) and subsurface rock (white)

All specific values for lengths and sizes are shown in the figure, with the exception of the radius of the domain which was not assigned a length. Steady state heat exchange modelling has been performed for this domain with the COMSOL[7] finite element tool. The computations only involved heat conduction. For this report results

---

[7] www.comsol.com

are presented for the specific geometry shown in Figure C.1, with the following temperature boundary conditions:

- Left, symmetry axis: zero flux
- Top: fixed temperature of 15 °C
- Bottom: fixed temperature of 195 °C
- Right: fixed temperature according to linear profile from top to bottom temperature with gradient of 30 °C/km,

and with the following conductivity values:

- Blue (brine): 0.6 W/m°C
- White (rock): 2.5 W/m°C
- Black (casing): 50 W/m°C

For the radius of the domain two values were chosen. In a first step this radius was set to a value of 1 km and with the consequence that the casing is such a small part that it is better not be given a representation with elements. Instead the casing was represented with a 1D-representation via the so-called thin layer option of COMSOL and via which only radial conductive heat exchange was accounted for (and vertical conductive heat exchange not taken into account). The mesh representation of COMSOL near the bottom of the well bore is shown in the left display in Figure C.2.
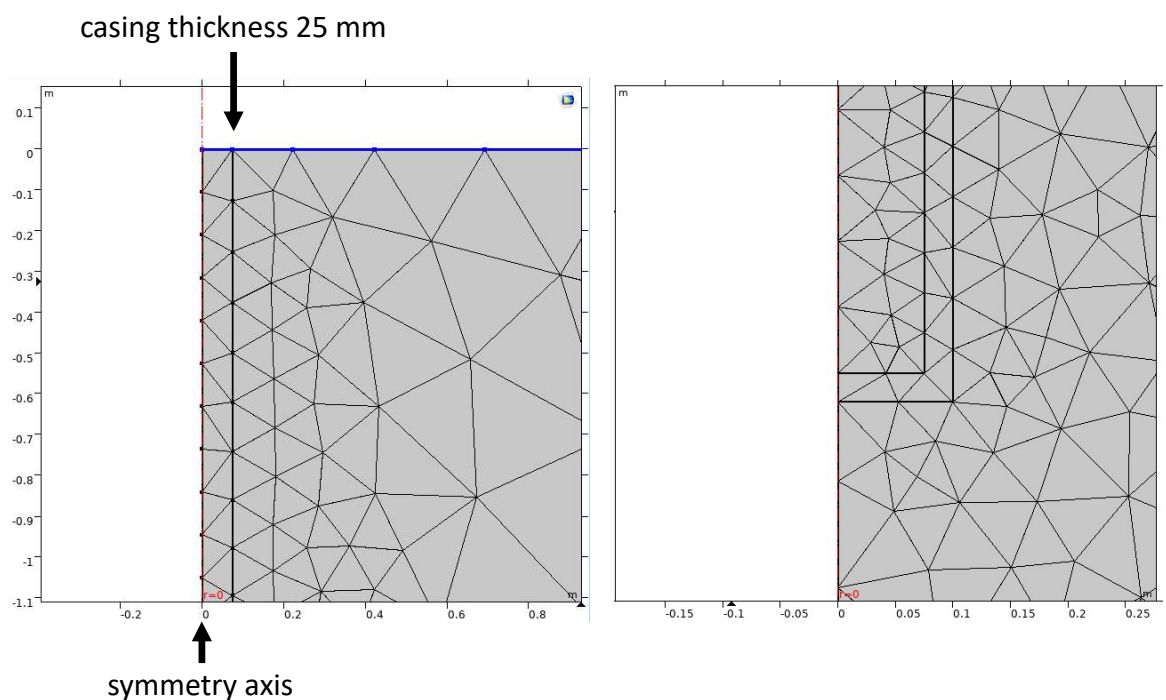

Figure C.2   Near well bore mesh representation for radius of 1 km (left) and 10 metres (right).

In a second step, and as an extra check on the results obtained in the first step, the radius was decreased to 10 metres. This reduction had as a consequence that the

casing could be represented with elements similar to those in the other parts of the domain, as shown via the mesh representation near the bottom of the wellbore in the right display in Figure C.2.

To conclude on the influence of the steel casing on the near wellbore temperature distribution it was opted to display the temperature along $z = 2999.9$ metres and for both calculation steps this is shown, left and right display, respectively, in Figure C.3. From this figure it is obvious that both distributions are very similar to each other, whereas both distributions also demonstrate that the temperature in the wellbore differs hardly from the reservoir temperature. Similar very small differences are seen at other depths. Hence, it is concluded from this characteristic setting that the influence of the steel casing on a temperature measurement obtained in a well is very limited for a steady state situation.
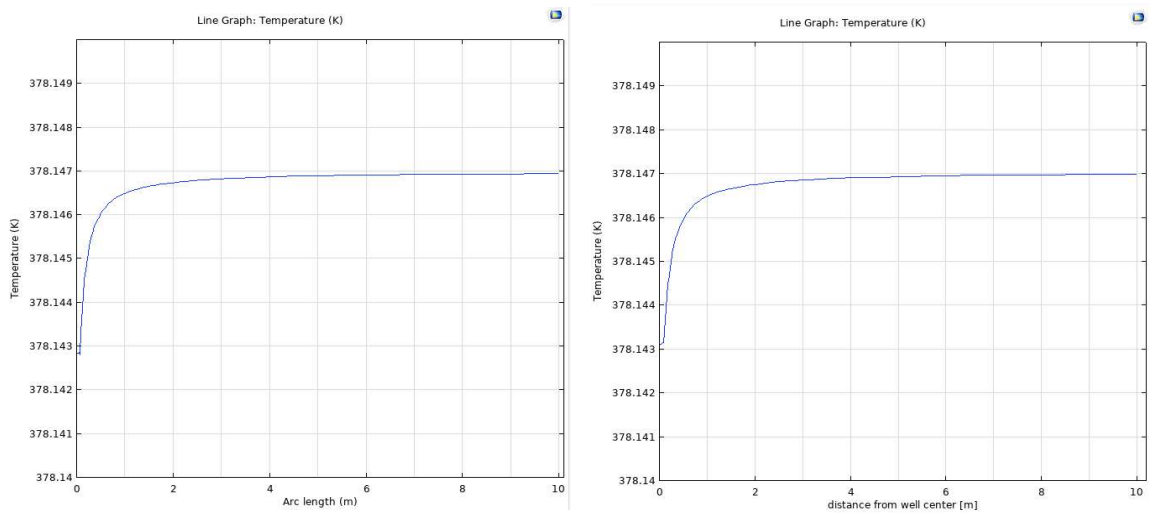

Figure C.3   Temperature distribution in °K near the well bore at $z = 2999.9$ metre for radius of 1 km (left) and 10 metre (right).

Onderzoek in de ondergrond voor aardwarmte